to the therapy or, indeed, whether bone destruction will be completely prevented by it. Recent progress in understanding the mechanism of bone loss in RA has provided promising new strategies, one of which is an anti-RANKL antibody directly suppressing RANKL-mediated osteoclastogenesis (51). As we have demonstrated a new role of Th17 in the context of bone damage in RA, the significance of the IL-23–IL-17 axis extends beyond the simple initiation or development of the autoimmunity. Because osteoclastogenic Th17 cells link the autoimmune inflammation to bone damage, inhibition of this axis has the potential of a doubly beneficial impact on RA, i.e., in the context of both the immune and skeletal systems, and thus appears to be an ideal therapeutic strategy for ameliorating the bone destruction associated with T cell activation.

MATERIALS AND METHODS

Mice. *Ifngr1*$^{-/-}$ (28), *Stat6*$^{-/-}$ (30), *Il17*$^{-/-}$ (37), and *Il23a*$^{-/-}$ mice (38) were described previously. All the mice were maintained under specific pathogen-free conditions and were backcrossed to C57BL/6 mice. All animal experiments were performed with the approval of the Animal Study Committee of Tokyo Medical and Dental University and conformed to relevant guidelines and laws.

Analysis of bone phenotype and LPS-induced bone destruction. The mice were subjected to histomorphometric and microradiographic examinations as described previously (27). 8-wk-old mice were injected with 25 mg/kg body weight LPS (Sigma-Aldrich) subperiosteally in the calvarial bone. After 5 d, calvarial bones were analyzed as described previously using decalcified paraffin sections (14).

In vitro assays for osteoclast differentiation and function. In vitro osteoclast differentiation was described previously (27, 52). For the RANKL–M-CSF system, we cultured BMCs with 10 ng/ml M-CSF (R&D Systems) for 2 d and used them as BMMs. The cells were cultured with 50 ng/ml RANKL (PeproTech) and 10 ng/ml M-CSF for 3 d, and $TRAP^+$ multinucleated (more than three nuclei) cells were counted. The co-culture of osteoblasts derived from mouse calvarial cells and BMCs was performed in the presence of 10^{-8} M $VitD_3$ (Wako) and 10^{-6} M PGE_2 (Wako) for 7 d. For the assessment of the bone-resorbing function of osteoclasts, we cultured osteoclast precursors on a hydroxy appatite–coated disc (Osteologic; BD Biosciences). After the culture period, the cells were washed away as described in the manufacturer's protocol by 6% NaOCl and 5.2% NaCl.

Th cell differentiation. $CD4^+$ T cells were purified from the spleen using a magnetic sorter and anti-CD4 microbeads (MACS; Miltenyi Biotec). The purity of the $CD4^+$ T cells was >95%. These $CD4^+$ T cells were stimulated with a plate-bound anti-CD3 mAb and anti-CD28 mAb (1 μg/ml each) for 3 d in the presence of (a) 10 ng/ml IL-12 and 10 μg/ml anti–IL-4 mAb for the Th1 cells, (b) 10 ng/ml IL-4 and 10 μg/ml anti–IFN-γ mAb for the Th2 cells, and (c) 10 ng/ml IL-23 along with 10 μg/ml each of anti–IFN-γ and anti–IL-4 mAbs for the Th17 cells. When indicated, the T cells were added to the culture system with 1 μg/ml anti-CD3 mAb for restimulation. All the antibodies were purchased from BD Biosciences except for the anti-RANKL mAb (provided by H. Yagita, Juntendo University School of Medicine, Tokyo, Japan). Recombinant IL-17 and the other cytokines were purchased from Genzyme and R&D Systems, respectively. T reg cells were purified using a MACS $CD4^-CD25^+$ Regulatory T Cell Isolation kit.

Analysis of mRNAs expressed in RA synovial tissues. Synovial tissues were obtained at the time of total knee arthroplasty from five patients (age range, 55–70 yr) who fulfilled the American College of Rheumatology criteria and gave informed consent (16). The experiments were performed with the approval of the institutional ethical committee. The tissues were minced and homogenized in Sepasol-RNA (Nacalai Tesque), and total RNA was extracted and purified according to the manufacturer's protocol.

GeneChip analysis and quantitative RT-PCR. Total RNA (15 μg) was used for cDNA synthesis by reverse transcription followed by the synthesis of biotinylated cRNA through in vitro transcription. After cRNA fragmentation, we performed hybridization with a mouse A430 GeneChip (Affymetrix, Inc.) (31). We performed quantitative RT-PCR using a LightCycler (Roche), as described previously (52). The following primers were used: *IL23A*: 5′-CTGCTTGCAAAGGATCCACC-3′ (sense), 5′-TTGAAGCGGAGAAGGAGACG-3′ (antisense); *IL12A*: 5′-AGCCTCCTCCTTGTGGCTA-3′ (sense), 5′-TGTGCTGGTTTTATCTTTTGTG-3′ (antisense); *IL12B*: 5′-TCACAAAGGAGGCGAGGTT-3′ (sense), 5′-ATGACCTCAATGGGCAGACTC-3′ (antisense); and *RANKL*: 5′-AACCAGATGGGATGTCGGTGGCATTA-3′ (sense), 5′-AGCGATGGTGGATGGCTCATGGTTAG-3′ (antisense). The level of mRNA expression was normalized with that of *GAPDH* expression in Fig. 5 A.

Statistical analyses. All data were expressed as the mean ± SEM ($n = 4$, unless otherwise indicated). Mann-Whitney U test was used for statistical analyses (*, $P < 0.05$; **, $P < 0.01$), and comparisons were made between each sample and the control (not treated with T cells/cytokines or WT mice).

Online supplemental material. Fig. S1 shows the effect of recombinant IL-4 on osteoclast precursor cells derived from WT or *Stat6*$^{-/-}$ mice in the RANKL–M-CSF system. Fig. S2 shows the list of genes whose expression was increased by IL-4 in osteoclast precursor cells (GeneChip analysis). Figs. S1 and S2 are available at http://www.jem.org/cgi/content/full/jem.20061775/DC1.

We are grateful to H. Yagita for providing anti-RANKL mAb. We also thank T. Taniguchi, S. Hida, S. Taki, H. Murayama, J. Taka, M. Asagiri, M. Shinohara, T. Nakashima, H.J. Gober, T. Koga, Y. Sato, and I. Takayanagi for fruitful discussion and assistance.

This work was supported in part by Grant-in-Aid for Creative Scientific Research from Japan Society for the Promotion of Science (JSPS), SORST program of JST, grants for Genome Network Project from the Ministry of Education, Culture, Sports, Science, and Technology of Japan (MEXT), grants for the 21st century COE program from MEXT, Grants-in-Aid for Scientific Research from MEXT, Health Sciences Research Grants from the Ministry of Health, Labor and Welfare of Japan, and grants from the Naito Foundation, Suzuken Memorial Foundation, Uehara Memorial Foundation, Kato Memorial Bioscience Foundation, Cell Science Research Foundation, Inamori Foundation, and the Nakatomi Foundation.

The authors have no conflicting financial interests.

Submitted: 18 August 2006
Accepted: 12 October 2006

REFERENCES

1. Walsh, M.C., N. Kim, Y. Kadono, J. Rho, S.Y. Lee, J. Lorenzo, and Y. Choi. 2006. Osteoimmunology: interplay between the immune system and bone metabolism. *Annu. Rev. Immunol.* 24:33–63.
2. Takayanagi, H. 2005. Inflammatory bone destruction and osteoimmunology. *J. Periodontal Res.* 40:287–293.
3. Sato, K., and H. Takayanagi. 2006. Osteoclasts, rheumatoid arthritis, and osteoimmunology. *Curr. Opin. Rheumatol.* 18:419–426.
4. Theill, L.E., W.J. Boyle, and J.M. Penninger. 2002. RANK-L and RANK: T cells, bone loss, and mammalian evolution. *Annu. Rev. Immunol.* 20:795–823.
5. Teitelbaum, S.L., and F.P. Ross. 2003. Genetic regulation of osteoclast development and function. *Nat. Rev. Genet.* 4:638–649.
6. Boyle, W.J., W.S. Simonet, and D.L. Lacey. 2003. Osteoclast differentiation and activation. *Nature.* 423:337–342.
7. Suda, T., N. Takahashi, N. Udagawa, E. Jimi, M.T. Gillespie, and T.J. Martin. 1999. Modulation of osteoclast differentiation and function by the new members of the tumor necrosis factor receptor and ligand families. *Endocr. Rev.* 20:345–357.

8. Mosmann, T.R., H. Cherwinski, M.W. Bond, M.A. Giedlin, and R.L. Coffman. 1986. Two types of murine helper T cell clone. I. Definition according to profiles of lymphokine activities and secreted proteins. *J. Immunol.* 136:2348–2357.
9. Dong, C. 2006. Diversification of T-helper-cell lineages: finding the family root of IL-17-producing cells. *Nat. Rev. Immunol.* 6:329–333.
10. Weaver, C.T., L.E. Harrington, P.R. Mangan, M. Gavrieli, and K.M. Murphy. 2006. Th17: an effector CD4 T cell lineage with regulatory T cell ties. *Immunity* 24:677–688.
11. Sakaguchi, S. 2005. Naturally arising Foxp3-expressing $CD25^{+}CD4^{+}$ regulatory T cells in immunological tolerance to self and non-self. *Nat. Immunol.* 6:345–352.
12. Takayanagi, H. 2005. Mechanistic insight into osteoclast differentiation in osteoimmunology. *J. Mol. Med.* 83:170–179.
13. Kong, Y.Y., U. Feige, I. Sarosi, B. Bolon, A. Tafuri, S. Morony, C. Capparelli, J. Li, R. Elliott, S. McCabe, et al. 1999. Activated T cells regulate bone loss and joint destruction in adjuvant arthritis through osteoprotegerin ligand. *Nature.* 402:304–309.
14. Takayanagi, H., K. Ogasawara, S. Hida, T. Chiba, S. Murata, K. Sato, A. Takaoka, T. Yokochi, H. Oda, K. Tanaka, et al. 2000. T-cell-mediated regulation of osteoclastogenesis by signalling cross-talk between RANKL and IFN-γ. *Nature.* 408:600–605.
15. Hofbauer, L.C., D.L. Lacey, C.R. Dunstan, T.C. Spelsberg, B.L. Riggs, and S. Khosla. 1999. Interleukin-1β and tumor necrosis factor-α, but not interleukin-6, stimulate osteoprotegerin ligand gene expression in human osteoblastic cells. *Bone.* 25:255–259.
16. Takayanagi, H., H. Iizuka, T. Juji, T. Nakagawa, A. Yamamoto, T. Miyazaki, Y. Koshihara, H. Oda, K. Nakamura, and S. Tanaka. 2000. Involvement of receptor activator of nuclear factor κB ligand/osteoclast differentiation factor in osteoclastogenesis from synoviocytes in rheumatoid arthritis. *Arthritis Rheum.* 43:259–269.
17. Dolhain, R.J., A.N. van der Heiden, N.T. ter Haar, F.C. Breedveld, and A.M. Miltenburg. 1996. Shift toward T lymphocytes with a T helper 1 cytokine-secretion profile in the joints of patients with rheumatoid arthritis. *Arthritis Rheum.* 39:1961–1969.
18. Smolen, J.S., M. Tohidast-Akrad, A. Gal, M. Kunaver, G. Eberl, P. Zenz, A. Falus, and G. Steiner. 1996. The role of T-lymphocytes and cytokines in rheumatoid arthritis. *Scand. J. Rheumatol.* 25:1–4.
19. Husby, G., and R.C. Williams Jr. 1985. Immunohistochemical studies of interleukin-2 and γ-interferon in rheumatoid arthritis. *Arthritis Rheum.* 28:174–181.
20. Kinne, R.W., E. Palombo-Kinne, and F. Emmrich. 1997. T-cells in the pathogenesis of rheumatoid arthritis villains or accomplices? *Biochim. Biophys. Acta.* 1360:109–141.
21. Manoury-Schwartz, B., G. Chiocchia, N. Bessis, O. Abehsira-Amar, F. Batteux, S. Muller, S. Huang, M.C. Boissier, and C. Fournier. 1997. High susceptibility to collagen-induced arthritis in mice lacking IFN-γ receptors. *J. Immunol.* 158:5501–5506.
22. Vermeire, K., H. Heremans, M. Vandeputte, S. Huang, A. Billiau, and P. Matthys. 1997. Accelerated collagen-induced arthritis in IFN-γ receptor-deficient mice. *J. Immunol.* 158:5507–5513.
23. Murphy, C.A., C.L. Langrish, Y. Chen, W. Blumenschein, T. McClanahan, R.A. Kastelein, J.D. Sedgwick, and D.J. Cua. 2003. Divergent pro- and antiinflammatory roles for IL-23 and IL-12 in joint autoimmune inflammation. *J. Exp. Med.* 198:1951–1957.
24. Nakae, S., A. Nambu, K. Sudo, and Y. Iwakura. 2003. Suppression of immune induction of collagen-induced arthritis in IL-17-deficient mice. *J. Immunol.* 171:6173–6177.
25. Kotake, S., N. Udagawa, N. Takahashi, K. Matsuzaki, K. Itoh, S. Ishiyama, S. Saito, K. Inoue, N. Kamatani, M.T. Gillespie, et al. 1999. IL-17 in synovial fluids from patients with rheumatoid arthritis is a potent stimulator of osteoclastogenesis. *J. Clin. Invest.* 103: 1345–1352.
26. Horwood, N.J., V. Kartsogiannis, J.M. Quinn, E. Romas, T.J. Martin, and M.T. Gillespie. 1999. Activated T lymphocytes support osteoclast formation *in vitro*. *Biochem. Biophys. Res. Commun.* 265: 144–150.
27. Koga, T., M. Inui, K. Inoue, S. Kim, A. Suematsu, E. Kobayashi, T. Iwata, H. Ohnishi, T. Matozaki, T. Kodama, et al. 2004. Costimulatory signals mediated by the ITAM motif cooperate with RANKL for bone homeostasis. *Nature.* 428:758–763.
28. Huang, S., W. Hendriks, A. Althage, S. Hemmi, H. Bluethmann, R. Kamijo, J. Vilcek, R.M. Zinkernagel, and M. Aguet. 1993. Immune response in mice that lack the interferon-γ receptor. *Science.* 259:1742–1745.
29. Huang, W., R.J. O'Keefe, and E.M. Schwarz. 2003. Exposure to receptor-activator of NFκB ligand renders pre-osteoclasts resistant to IFN-γ by inducing terminal differentiation. *Arthritis Res. Ther.* 5:R49–R59.
30. Takeda, K., T. Tanaka, W. Shi, M. Matsumoto, M. Minami, S. Kashiwamura, K. Nakanishi, N. Yoshida, T. Kishimoto, and S. Akira. 1996. Essential role of Stat6 in IL-4 signalling. *Nature.* 380:627–630.
31. Takayanagi, H., S. Kim, T. Koga, H. Nishina, M. Isshiki, H. Yoshida, A. Saiura, M. Isobe, T. Yokochi, J. Inoue, et al. 2002. Induction and activation of the transcription factor NFATc1 (NFAT2) integrate RANKL signaling in terminal differentiation of osteoclasts. *Dev. Cell.* 3:889–901.
32. Asagiri, M., K. Sato, T. Usami, S. Ochi, H. Nishina, H. Yoshida, I. Morita, E.F. Wagner, T.W. Mak, E. Serfling, and H. Takayanagi. 2005. Autoamplification of NFATc1 expression determines its essential role in bone homeostasis. *J. Exp. Med.* 202:1261–1269.
33. Harrington, L.E., R.D. Hatton, P.R. Mangan, H. Turner, T.L. Murphy, K.M. Murphy, and C.T. Weaver. 2005. Interleukin 17-producing $CD4^{+}$ effector T cells develop via a lineage distinct from the T helper type 1 and 2 lineages. *Nat. Immunol.* 6:1123–1132.
34. Park, H., Z. Li, X.O. Yang, S.H. Chang, R. Nurieva, Y.H. Wang, Y. Wang, L. Hood, Z. Zhu, Q. Tian, and C. Dong. 2005. A distinct lineage of CD4 T cells regulates tissue inflammation by producing interleukin 17. *Nat. Immunol.* 6:1133–1141.
35. Mangan, P.R., L.E. Harrington, D.B. O'Quinn, W.S. Helms, D.C. Bullard, C.O. Elson, R.D. Hatton, S.M. Wahl, T.R. Schoeb, and C.T. Weaver. 2006. Transforming growth factor-β induces development of the T_H17 lineage. *Nature.* 441:231–234.
36. Bettelli, E., Y. Carrier, W. Gao, T. Korn, T.B. Strom, M. Oukka, H.L. Weiner, and V.K. Kuchroo. 2006. Reciprocal developmental pathways for the generation of pathogenic effector T_H17 and regulatory T cells. *Nature.* 441:235–238.
37. Nakae, S., Y. Komiyama, A. Nambu, K. Sudo, M. Iwase, I. Homma, K. Sekikawa, M. Asano, and Y. Iwakura. 2002. Antigen-specific T cell sensitization is impaired in IL-17-deficient mice, causing suppression of allergic cellular and humoral responses. *Immunity.* 17:375–387.
38. Cua, D.J., J. Sherlock, Y. Chen, C.A. Murphy, B. Joyce, B. Seymour, L. Lucian, W. To, S. Kwan, T. Churakova, et al. 2003. Interleukin-23 rather than interleukin-12 is the critical cytokine for autoimmune inflammation of the brain. *Nature.* 421:744–748.
39. Ukai, T., Y. Hara, and I. Kato. 1996. Effects of T cell adoptive transfer into nude mice on alveolar bone resorption induced by endotoxin. *J. Periodontal Res.* 31:414–422.
40. Gravallese, E.M., C. Manning, A. Tsay, A. Naito, C. Pan, E. Amento, and S.R. Goldring. 2000. Synovial tissue in rheumatoid arthritis is a source of osteoclast differentiation factor. *Arthritis Rheum.* 43: 250–258.
41. Pettit, A.R., H. Ji, D. von Stechow, R. Muller, S.R. Goldring, Y. Choi, C. Benoist, and E.M. Gravallese. 2001. TRANCE/RANKL knockout mice are protected from bone erosion in a serum transfer model of arthritis. *Am. J. Pathol.* 159:1689–1699.
42. Redlich, K., S. Hayer, R. Ricci, J.P. David, M. Tohidast-Akrad, G. Kollias, G. Steiner, J.S. Smolen, E.F. Wagner, and G. Schett. 2002. Osteoclasts are essential for TNF-α-mediated joint destruction. *J. Clin. Invest.* 110:1419–1427.
43. Horwood, N.J., J. Elliott, T.J. Martin, and M.T. Gillespie. 2001. IL-12 alone and in synergy with IL-18 inhibits osteoclast formation *in vitro*. *J. Immunol.* 166:4915–4921.
44. Udagawa, N., N.J. Horwood, J. Elliott, A. Mackay, J. Owens, H. Okamura, M. Kurimoto, T.J. Chambers, T.J. Martin, and M.T. Gillespie. 1997. Interleukin-18 (interferon-γ-inducing factor) is produced by osteoblasts and acts via granulocyte/macrophage colony-stimulating factor and not via interferon-γ to inhibit osteoclast formation. *J. Exp. Med.* 185:1005–1012.

45. Hong, M.H., H. Williams, C.H. Jin, and J.W. Pike. 2000. The inhibitory effect of interleukin-10 on mouse osteoclast formation involves novel tyrosine-phosphorylated proteins. *J. Bone Miner. Res.* 15:911–918.
46. Kadono, Y., F. Okada, C. Perchonock, H.D. Jang, S.Y. Lee, N. Kim, and Y. Choi. 2005. Strength of TRAF6 signalling determines osteoclastogenesis. *EMBO Rep.* 6:171–176.
47. Gohda, J., T. Akiyama, T. Koga, H. Takayanagi, S. Tanaka, and J. Inoue. 2005. RANK-mediated amplification of TRAF6 signaling leads to NFATc1 induction during osteoclastogenesis. *EMBO J.* 24: 790–799.
48. Hikita, A., Y. Kadono, H. Chikuda, A. Fukuda, H. Wakeyama, H. Yasuda, K. Nakamura, H. Oda, T. Miyazaki, and S. Tanaka. 2005. Identification of an alternatively spliced variant of Ca^{2+}-promoted Ras inactivator as a possible regulator of RANKL shedding. *J. Biol. Chem.* 280:41700–41706.
49. Ross, F.P., and S.L. Teitelbaum. 2005. αvβ3 and macrophage colony-stimulating factor: partners in osteoclast biology. *Immunol. Rev.* 208: 88–105.
50. Palladino, M.A., F.R. Bahjat, E.A. Theodorakis, and L.L. Moldawer. 2003. Anti-TNF-α therapies: the next generation. *Nat. Rev. Drug Discov.* 2:736–746.
51. McClung, M.R., E.M. Lewiecki, S.B. Cohen, M.A. Bolognese, G.C. Woodson, A.H. Moffett, M. Peacock, P.D. Miller, S.N. Lederman, C.H. Chesnut, et al. 2006. Denosumab in postmenopausal women with low bone mineral density. *N. Engl. J. Med.* 354:821–831.
52. Kim, Y., K. Sato, M. Asagiri, I. Morita, K. Soma, and H. Takayanagi. 2005. Contribution of nuclear factor of activated T cells c1 to the transcriptional control of immunoreceptor osteoclast-associated receptor but not triggering receptor expressed by myeloid cells-2 during osteoclastogenesis. *J. Biol. Chem.* 280:32905–32913.

Cell

Force Sensing by Mechanical Extension of the Src Family Kinase Substrate p130Cas

Yasuhiro Sawada,[1,*] Masako Tamada,[1] Benjamin J. Dubin-Thaler,[1] Oksana Cherniavskaya,[1] Ryuichi Sakai,[2] Sakae Tanaka,[3] and Michael P. Sheetz[1]
[1] Department of Biological Sciences, Columbia University, Sherman Fairchild Center Room 715, MC-2416, 1212 Amsterdam Avenue, New York, NY 10027, USA
[2] Growth Factor Division, National Cancer Center Research Institute, 5-1-1 Tsukiji, Chuo-ku, Tokyo 104-0045, Japan
[3] Department of Orthopaedic Surgery, Graduate School of Medicine, The University of Tokyo, 7-3-1 Hongo, Bunkyo-ku, Tokyo 113-0033, Japan
*Contact: ys454-ind@umin.ac.jp
DOI 10.1016/j.cell.2006.09.044

SUMMARY

How physical force is sensed by cells and transduced into cellular signaling pathways is poorly understood. Previously, we showed that tyrosine phosphorylation of p130Cas (Cas) in a cytoskeletal complex is involved in force-dependent activation of the small GTPase Rap1. Here, we mechanically extended bacterially expressed Cas substrate domain protein (CasSD) in vitro and found a remarkable enhancement of phosphorylation by Src family kinases with no apparent change in kinase activity. Using an antibody that recognized extended CasSD in vitro, we observed Cas extension in intact cells in the peripheral regions of spreading cells, where higher traction forces are expected and where phosphorylated Cas was detected, suggesting that the in vitro extension and phosphorylation of CasSD are relevant to physiological force transduction. Thus, we propose that Cas acts as a primary force sensor, transducing force into mechanical extension and thereby priming phosphorylation and activation of downstream signaling.

INTRODUCTION

Cellular responses to mechanical force underlie many critical functions, from normal morphogenesis to carcinogenesis, cardiac hypertrophy, wound healing, and bone homeostasis. Recent studies indicate that various signaling pathways are involved in force transduction, including MAP kinases, small GTPases, and tyrosine kinases/phosphatases (Geiger and Bershadsky, 2002; Giannone and Sheetz, 2006; Katsumi et al., 2002; Sawada et al., 2001). A variety of primary force-sensing mechanisms could be postulated, including mechanical extension of cytoplasmic proteins, activation of ion channels, and formation of force-stabilized receptor-ligand bonds (catch bonds) (Vogel and Sheetz, 2006), which would then activate downstream signaling pathways. At a biochemical level, tyrosine phosphorylation levels appear to be linked to mechanically induced changes controlling many other cellular functions (Giannone and Sheetz, 2006). One protein involved in mechanically induced phosphorylation-dependent signaling is the Src family kinase substrate Cas (Crk-associated substrate), which is involved in various cellular events such as migration, survival, transformation, and invasion (Defilippi et al., 2006). Stretch-dependent tyrosine phosphorylation of Cas by Src family kinases (SFKs) occurs in detergent-insoluble cytoskeletal complexes and is involved in force-dependent activation of the small GTPase Rap1 (Tamada et al., 2004). Rap1 is activated by distinct types of guanine nucleotide exchange factors coupled with various receptors or second messengers and plays an important role in a number of signaling pathways, including integrin signaling (Hattori and Minato, 2003).

The Cas substrate domain, which is located in the center of Cas, is flanked by the amino-terminal SH3 and the carboxy-terminal Src-binding domains. These amino- and carboxy-terminal domains are involved in Cas localization at focal adhesions, while the substrate domain itself is not (Nakamoto et al., 1997), suggesting that these flanking domains anchor Cas molecules to the cytoskeletal complex and that the substrate domain could be extended upon cytoskeleton stretching. Furthermore, the Cas substrate domain has 15 repeats of a tyrosine-containing motif (YxxP) (Mayer et al., 1995), and multiple sequence repeats are found in molecules with mechanical functions such as titin (Rief et al., 1997).

Cell stretching could increase tyrosine phosphorylation by (1) directly activating the kinase, (2) inactivating the phosphatase, (3) mechanically bringing the kinase to the substrate, or (4) enhancing the susceptibility of the substrate to phosphorylation. To test between these possibilities, we have analyzed the mechanisms of stretch-dependent

enhancement of Cas phosphorylation. In intact cells, Cas phosphorylation by c-Src is significantly increased by cell stretching with no detectable change in c-Src kinase activity. Cas phosphorylation mediates physiological force transduction through stretch-dependent activation of Rap1 in intact cells. With *in vitro protein extension* (IPE) experiments, we find that phosphorylation of CasSD by specific kinases is increased upon extension. Further, an antibody that recognizes extended CasSD in vitro preferentially recognizes Cas molecules at the periphery of late spreading cells where higher traction forces are predicted and Cas is phosphorylated, indicating that the in vitro extension and phosphorylation of CasSD is relevant to force transduction through Cas phosphorylation in intact cells. Thus, we suggest that Cas serves as a direct mechanosensor where force induces a mechanical extension of the substrate domain that primes it for phosphorylation. We propose that such "substrate priming" is a general mechanism for force transduction.

RESULTS

Cell Stretching Enhances SFK-Dependent Phosphorylation of Cas without a Detectable Increase in Src Kinase Activity

We first examined whether the phosphorylation of Cas increased upon intact cell stretching, using the cell stretching system that we developed (Sawada et al., 2001). Cells were cultured on a stretchable substrate (collagen-coated silicone), and the substrate was stretched uniformly and biaxially (10% in each dimension) and held stretched. To analyze the primary responses to cell stretching, samples were prepared from the cells lysed shortly (1 min) after stretching. Immunoblotting using an anti-phospho-Cas antibody (pCas-165) that specifically recognizes multiple phosphorylated YxxP motifs in the substrate domain (Fonseca et al., 2004) revealed a stretch-dependent increase in tyrosine phosphorylation of Cas in HEK293 cells (Figure 1A). When the selective SFK inhibitor CGP77675 (Missbach et al., 1999) (Novartis Pharma AG, Switzerland) was added prior to stretching, stretch-dependent tyrosine phosphorylation of Cas was inhibited (Figure 1A). Furthermore, stretch-dependent phosphorylation of Cas was greatly attenuated in SYF cells that lacked the major SFKs, c-Src, c-Yes, and Fyn (Klinghoffer et al., 1999), and was restored in SYF cells stably expressing c-Src (Figure 1B), c-Yes, or Fyn (data not shown). Thus, stretching intact cells increased tyrosine phosphorylation of Cas by SFKs.

To determine if stretch-dependent increases in Cas phosphorylation correlated with SFK activation, the levels of c-Src phosphorylation at either activating or inhibiting tyrosine residue (Y416 and Y527, respectively) were examined in SYF cells stably expressing c-Src, either stretched or left unstretched. We observed no changes in phosphorylation levels of those tyrosines (pY416 and pY527) (Figure 1B, lanes 3 and 4). Since the levels of pY416 and pY527 indicate Src kinase inhibition and activation, respectively (Thomas and Brugge, 1997), cell stretching did not appear to affect c-Src activity, while Cas phosphorylation significantly increased. This was further confirmed by an in vitro kinase assay of immunoprecipitated c-Src (Figure 1C). Thus, stretching intact cells increased tyrosine phosphorylation of Cas by c-Src without detectable enhancement of c-Src kinase activity.

Tyrosine Phosphorylation of Cas Is Involved in Stretch-Dependent Rap1 Activation

To explore the role of Cas in physiological force transduction pathways, we analyzed the involvement of Cas in the stretch-dependent activation of Rap1 in cells (Sawada et al., 2001). When the level of Cas protein and phosphorylated Cas was selectively decreased by small interfering RNA (siRNA) in HEK293 cells (Figure 2A, upper panel), Rap1 activity in cells, either stretched or unstretched, was significantly attenuated (Figure 2A, lower panel). Thus, Cas plays a significant role in the stretch-dependent activation of Rap1 in intact cells. However, there is likely more than one pathway for Rap1 activation, considering the fold decrease of Rap1 activity (~50%) in Cas knockdown cells (Figure 2A) as well as the stretch-dependent Rap1 activation observed in Cas-deficient fibroblasts (data not shown).

To further examine the role of phosphorylation of Cas in stretch-dependent Rap1 activation, we overexpressed Cas together with Rap1 in HEK293 cells. Upon coexpression of monomeric red fluorescent protein (RFP)-tagged wild-type Cas (RFP-Cas) with green fluorescent protein (GFP)-tagged Rap1 (GFP-Rap1), stretch-dependent activity of GFP-Rap1 was enhanced over the cells coexpressing RFP alone or RFP-Cas15YF that had all 15 YxxP motifs in the substrate domain mutated to FxxP (Figure 2B). The fold increase of Rap1 activity by cell stretching appeared to be smaller in the case of RFP-Cas-expressing cells, probably due to the less efficient incorporation of "overexpressed" Cas into physiological signaling complexes. However, we conclude that tyrosine phosphorylation of Cas is responsible for a significant fraction of the stretch-dependent Rap1 activation.

In Vitro Extension of CasSD

Because kinase activation did not appear to be the primary mechanism regulating Cas phosphorylation in response to cell stretching (Figures 1B and 1C), we tested whether the mechanical extension of the Cas substrate domain modulated its susceptibility to phosphorylation by SFKs. To eliminate the involvement of any extraneous molecules, we performed biochemical analysis, using an IPE system. In that system, bacterially expressed Cas substrate domain protein, CasSD (Cas115–420), was biotinylated on both amino and carboxy termini (designated NC-biotinylated CasSD, Figure 3A, top) and was bound to avidin covalently immobilized on a latex substrate (Figure 3A). After stretching of the latex membrane (Figure 3A), biochemical analyses were performed.

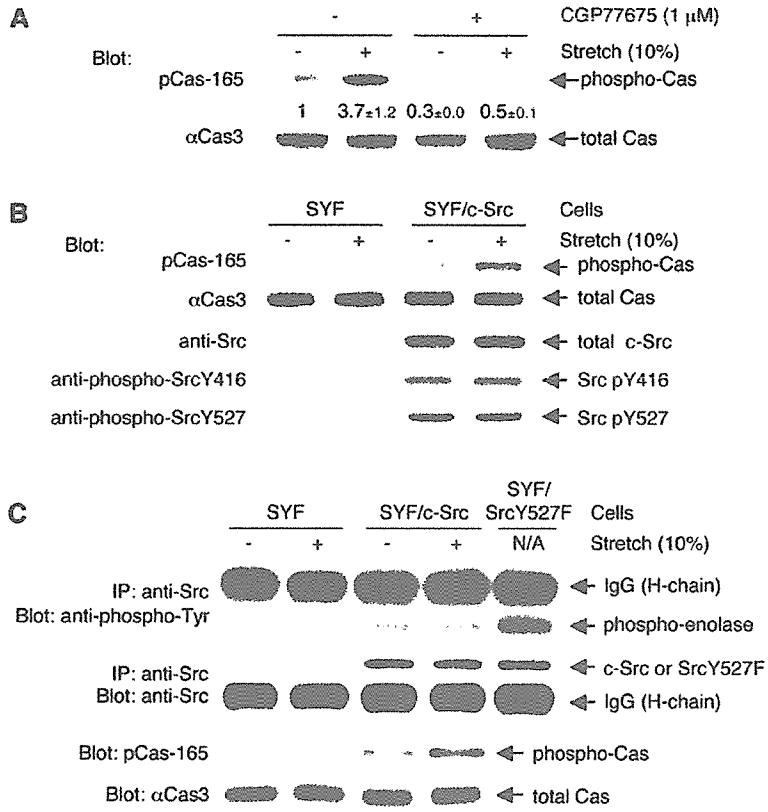

Figure 1. SFK- and Stretch-Dependent Tyrosine Phosphorylation of Cas In Vivo

(A) Stretch-dependent tyrosine phosphorylation of Cas in intact cells. HEK293 (2×10^5) cells on the collagen (type I)-coated stretchable silicone dish were treated with either CGP77675 (1 μM) or its vehicle (0.01% DMSO) and were either stretched (biaxially, 10% in each dimension) or left unstretched. One minute after stretching or without stretching, the cells were solubilized with 1× SDS sample buffer containing 20 mM DTT and analyzed for Cas phosphorylation by anti-phospho-Cas (pCas-165) and anti-Cas (αCas3) immunoblotting. Quantification of phosphorylation (phospho-Cas/total Cas) was scaled with unstretched control set at 1 and noted below the pCas-165 blot with SD ($n = 4$).

(B) Cell stretching increases Src-dependent phosphorylation of Cas without apparent change in phosphorylation levels of activating and inhibiting tyrosines of c-Src. SYF cells (triple knockout cells of c-src, c-yes, and fyn) or SYF cells stably expressing c-Src (4×10^5) were either stretched or left unstretched. One minute after stretching or without stretching, cells were solubilized with SDS sample buffer, and equivalent portions of each sample were subjected to SDS-PAGE followed by pCas-165, αCas3, anti-Src, anti-phospho-Src Y416, and anti-phospho-Src Y527 immunoblotting.

(C) Cell stretching increases Src-dependent phosphorylation of Cas without apparent change in Src kinase activity. SYF cells or SYF cells stably expressing c-Src (4×10^5) were either stretched or left unstretched. One minute after stretching or without stretching, cells were lysed and subjected to immunoprecipitation followed by an in vitro kinase assay using acid-treated enolase as a substrate. Src kinase activity was analyzed by measuring the phosphorylation of enolase with anti-phospho-tyrosine immunoblotting (top panel). Immunoprecipitated Src, i.e., Src protein in the kinase reaction, was quantified by anti-Src immunoblotting (second panel). Equivalent small portions of each lysate were mixed with SDS sample buffer and subjected directly to SDS-PAGE followed by pCas-165 and αCas3 immunoblotting to analyze for Cas phosphorylation (third and fourth panels). Kinase reactions for the lane 3 and 4 samples appeared not to be saturated because the sample prepared from SYF/SrcY527F cells (SYF cells expressing SrcY527F, the highly active mutant form of c-Src) cultured on a plastic plate following the same protocol gave more phosphorylation of enolase (lane 5). The intense bands above enolase (top panel) and below Src (second panel) represent IgG (heavy chain) from the anti-Src antibody.

To determine if stretching of the latex membrane actually extended NC-biotinylated CasSD, we developed the yellow fluorescent protein (YFP) amino-terminal swapping assay based on the interaction between the amino- and carboxy-terminal regions of YFP. In this assay, CasSD extension was detected by the separation of YFP components attached to the ends of CasSD, causing the binding of an exogenous YFP component. When the two halves of a split YFP, YFP-N and YFP-C, were fused to the amino- and carboxy-terminal ends of NC-biotinylated CasSD, respectively (NY/CY-NC-biotinylated CasSD, Figure 3B), we observed yellow fluorescence in both NY/CY-NC-biotinylated CasSD-expressing bacteria and the purified protein, as expected (Hu et al., 2002). When we added purified His_6-YFP-N to bind to YFP-C in NY/CY-NC biotinylated CasSD (Figure 3B, top), His_6-YFP-N binding was not observed without latex membrane stretching (Figure 3C, lane 1). However, we observed His_6-YFP-N binding upon stretching (Figure 3C, lane 2). Furthermore, His_6-YFP-N did not bind to NY/CY-C-biotinylated CasSD (the unextendable mono-biotinylated control, Figure 3B, bottom) or NC-biotinylated CasSD (extendable, but with no YFP component, Figure 3A, top) even following stretching (Figure 3C, lanes 3–6). Using His_6-YFP-N together with YFP-C fused to glutathione *S*-transferase (GST) in a GST pull-down experiment, we found that YFP-N bound to YFP-C under the same buffer conditions used in the YFP amino-terminal swapping assay (data not shown). Thus, stretching of the latex membrane separated the YFP halves in NY/CY-NC-biotinylated CasSD and allowed His_6-YFP-N to bind, indicating the extension of CasSD (Figure 3B, top).

Extension-Dependent Phosphorylation of CasSD by Recombinant Tyrosine Kinases In Vitro

Since CasSD could be extended by the IPE system, we examined the effect of extension on tyrosine phosphorylation of CasSD by recombinant active c-Src. While the level of phosphorylation was low without stretching (Figure 4A, lane 1), CasSD phosphorylation increased in proportion

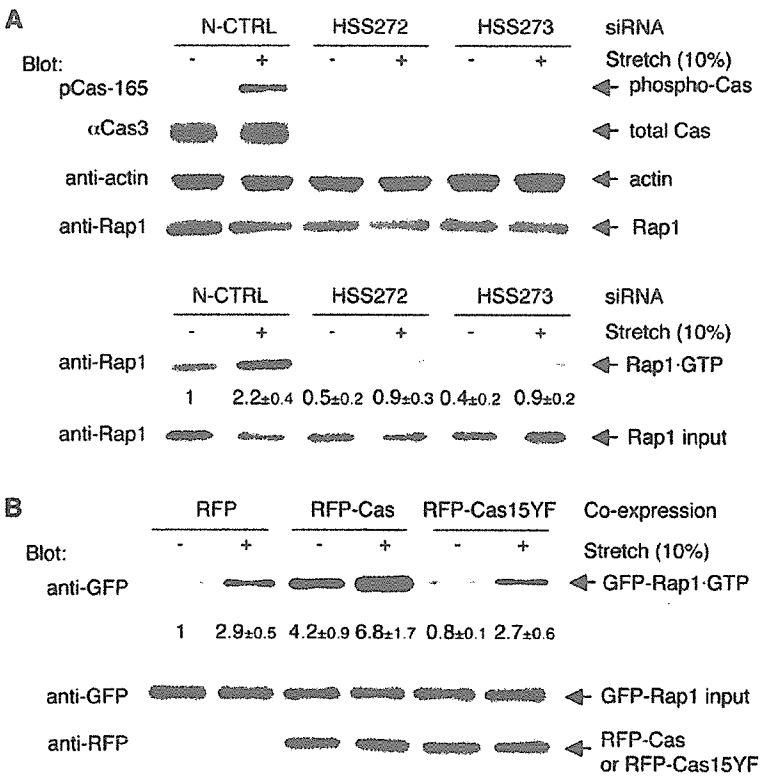

Figure 2. Significant Role of Cas Phosphorylation in Physiological Force Transduction

(A) Cas is involved in stretch-dependent Rap1 activation in intact cells. RNAi experiments were performed as described in the Experimental Procedures. siRNAs used were Stealth RNAi Negative Control Med GC (N-CTRL: lanes 1 and 2), BCAR1-HSS114272 (HSS272: lanes 3 and 4), and BCAR1-HSS114273 (HSS273: lanes 5 and 6) (Invitrogen). Twenty-four hours after transfection, HEK293 cells were either stretched or left unstretched. To determine the level of Cas expression and phosphorylation, cells were solubilized with SDS sample buffer 1 min after stretching or without stretching, and equivalent portions of each sample were subjected to SDS-PAGE followed by anti-phospho-Cas (pCas-165), anti-Cas (αCas3), anti-Rap1, and anti-actin immunoblotting (upper panel). To measure stretch-dependent Rap1 activity, cells were solubilized with lysis buffer for GST pull-down assay (see Experimental Procedures) 5 min after stretching or without stretching. Rap1 was quantified by anti-Rap1 immunoblotting. Rap1 activity (Rap1•GTP/Rap1 input) was scaled with the unstretched control set at 1 and noted below the Rap1•GTP blot with SD (n = 4) (lower panel). The data shown in Figure 2A (upper and lower panels) were obtained with siRNA transfection performed at the same time.

(B) Significant role of tyrosine phosphorylation of Cas in stretch-dependent Rap1 activation. RFP, RFP-Cas, or RFP-Cas15YF was cotransfected with GFP-Rap1 into HEK293 cells (1×10^5/dish). Twenty-four hours after transfection, cells were either stretched or left unstretched. Five minutes after stretching or without stretching, cells were solubilized and subjected to the GST pull-down assay. GFP-Rap1 was quantified by anti-GFP immunoblotting. GFP-Rap1 activity (GFP-Rap1•GTP/GFP-Rap1 input) was scaled with the unstretched RFP-transfected cells set at 1 and noted below the GFP-Rap1•GTP blot with SD (n = 4).

to the magnitude of latex membrane stretching (25%, 50%, 75%, 100%, and 150%) (Figure 4A, lanes 2–6). An unextendable mono-biotinylated CasSD (C-biotinylated CasSD, see Figure 3A, top) was poorly tyrosine phosphorylated either with or without stretching (Figure 4A, lanes 7 and 8). To test if c-Src kinase activity was modulated in the IPE experiments, we added acid-treated enolase to the kinase mixture at the time of kinase reaction and measured its phosphorylation. In the same reaction that gave an extension-dependent increase in CasSD phosphorylation, neither the level of enolase phosphorylation nor the phosphorylation levels of Y416 and Y527 of c-Src kinase were affected by stretching (data not shown). These results indicated that extension-dependent tyrosine phosphorylation of CasSD resulted from CasSD extension and not from an increase in the kinase activity of recombinant c-Src.

We also asked whether or not other kinases phosphorylated CasSD in an extension-dependent manner in IPE experiments. Neither the non-SFK tyrosine kinase Csk (C-terminal Src kinase) nor ZAP-70 phosphorylated NC-biotinylated CasSD, even after stretching (Figure 4B). However, in the same kinase reaction protocol, both Csk and ZAP-70 were able to phosphorylate their known substrates, acid-treated enolase (Bougeret et al., 1993) and the cytoplasmic fragment of human erythrocyte band 3 (cdb3) (Isakov et al., 1996), respectively (data not shown). On the other hand, a known Cas kinase, Abl (Mayer et al., 1995) and another SFK, FynT, phosphorylated CasSD in an extension-dependent manner (Figure 4B). Thus, extension-dependent phosphorylation of CasSD in vitro is caused in a kinase-specific manner, and not by a nonspecific effect of the IPE system.

Although neither the force needed for CasSD extension nor its effect on individual YxxP motifs in CasSD is known, the IPE experiments revealed that different extents of extension induced the phosphorylation of different regions. When we used two different anti-phospho-Cas antibodies (pCas-165 and pCas-410) that had different, though not strictly specific, binding preferences for YxxPs in the Cas substrate domain (Shin et al., 2004) to measure the in vitro CasSD phosphorylation, pCas-410 immunoblotting gave significantly greater fold increase than pCas-165 blots by 40% latex membrane stretching (Figure 4C, left panel). However, pCas-165 and pCas-410 blots showed a similar fold increase by 100% stretching (Figure 4C, right panel). These results suggest that the pCas-410 sites are more efficiently exposed and phosphorylated than pCas-165 sites by smaller extent of CasSD extension.

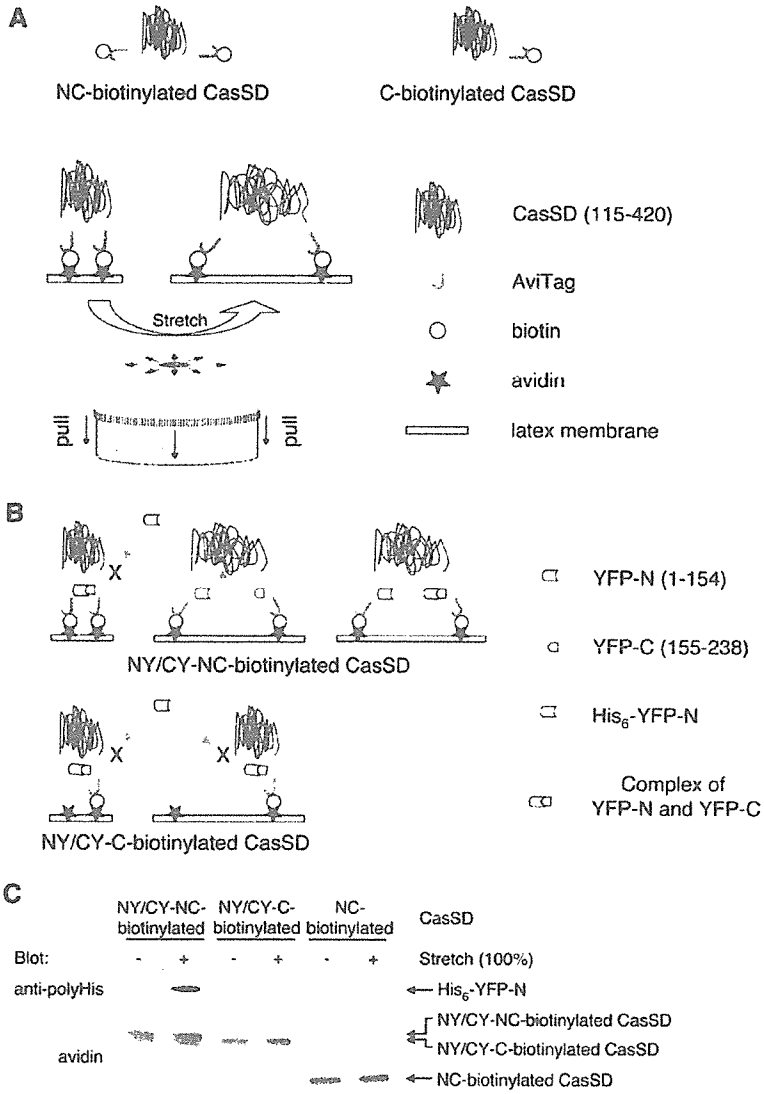

Figure 3. IPE System

(A) Scheme of NC-biotinylated CasSD, C-biotinylated CasSD, and the process of mechanical extension of CasSD in the IPE system.

(B) Schematic description of YFP amino-terminal swapping.

(C) His_6-YFP-N binds to extended NY/CY-NC-biotinylated CasSD, but not to NY/CY-C-biotinylated CasSD or NC-biotinylated CasSD. Biotinylated CasSD proteins, either extended or unextended on latex membrane, were incubated with His_6-YFP-N in the buffer containing 1% Triton X-100 and 1% BSA. After washing, bound complex was solubilized and subjected to SDS-PAGE followed by anti-polyHistidine immunoblotting or avidin affinity blotting.

αCas1, an Antibody that Recognizes Extended CasSD

In order to test if Cas was extended in regions of cell traction forces, we utilized an antibody, αCas1, which was raised against a peptide sequence in the Cas substrate domain (Sakai et al., 1994) (Figure S1A). We found that αCas1 recognized the extended NC-biotinylated CasSD and not the unextended control, C-biotinylated CasSD in the IPE system (Figure 5A). Further, αCas1 bound to SDS-denatured CasSD regardless of its phosphorylation state (Figure S1B), as well as full-length Cas in the SDS-denatured cell lysates (Figure S1C). Thus, αCas1 binding appeared to require the exposure of its epitope in the Cas substrate domain by either extension or denaturation.

Extension of Cas in Triton Cytoskeletons

Using αCas1, we examined whether Cas was extended by stretching Triton cytoskeletons where tyrosine phosphorylation of Cas was observed (Tamada et al., 2004). When we stretched Triton cytoskeletons from Cas-deficient fibroblasts expressing RFP-Cas, we observed a significant increase in αCas1 binding (Figure 5B, lower panel, lanes 1 and 2). Triton cytoskeletons from Cas-deficient fibroblasts expressing RFP alone did not bind αCas1 (Figure 5B, lower panel, lanes 3 and 4). Further, another anti-Cas antibody, αCas3, the epitope of which did not involve the substrate domain (Figure S1A) (Sakai et al., 1994), did not change its binding to Cas in Triton cytoskeletons upon stretching (Figure 5B, lower panel, lanes 5 and 6). These results indicate that the extension of the Cas substrate domain is enhanced by cytoskeleton stretching.

Cas Is Extended at the Sites of High Traction Forces Where Cas Is Phosphorylated In Vivo

Cas extension was difficult to observe in intact cells, since the cell stretching system could not fit onto a total internal

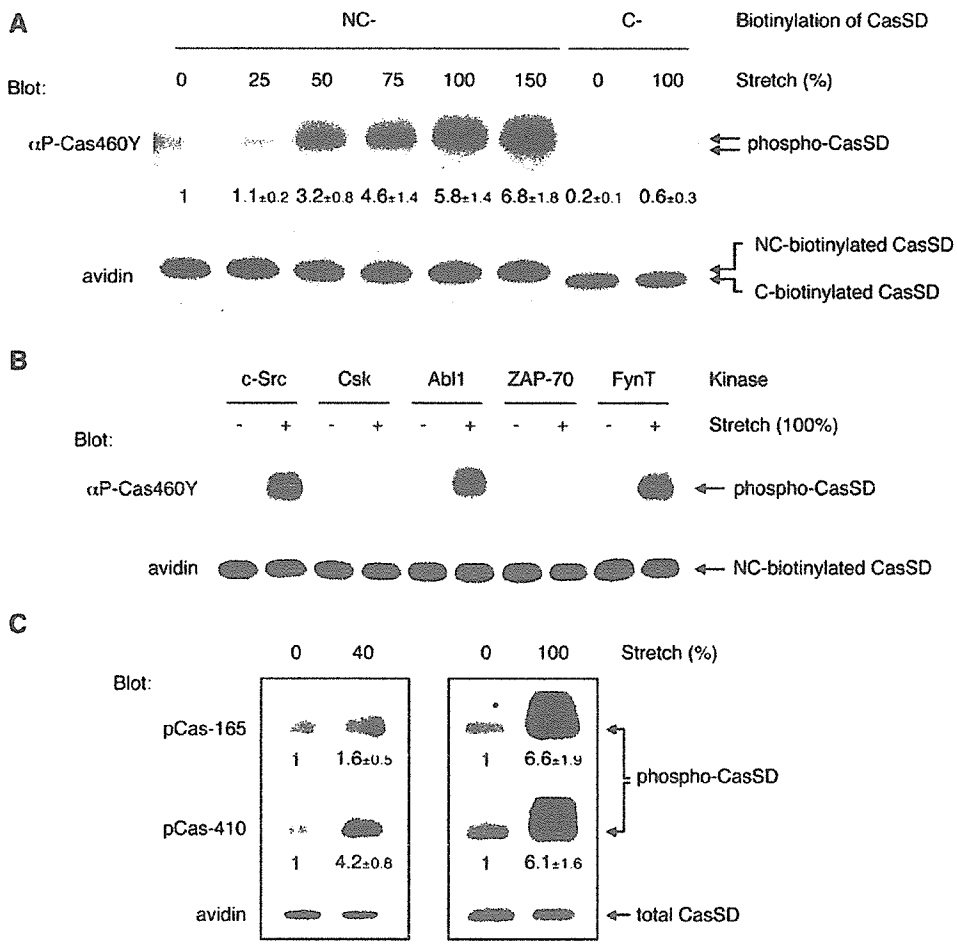

Figure 4. Extension-Dependent Phosphorylation of CasSD by Tyrosine Kinases In Vitro

(A) CasSD is tyrosine phosphorylated by recombinant c-Src in an extension-dependent manner. NC-biotinylated or C-biotinylated CasSD was either extended or left unextended on latex membrane, incubated with recombinant c-Src for 2 min, washed, solubilized, and analyzed for tyrosine phosphorylation by anti-phospho-Cas (αP-Cas460Y) immunoblotting and avidin affinity blotting. The magnitude of the latex membrane stretching is described as the percent change of length in each dimension. Quantification of phosphorylation of CasSD was scaled with unextended NC-biotinylated CasSD set at 1 and noted below the anti-phospho-Cas blot with SD (n = 4).

(B) Kinase specificity of extension-dependent tyrosine phosphorylation of CasSD. NC-biotinylated CasSD was either extended (100%) or left unextended and then incubated with recombinant c-Src, Csk, Abl1, ZAP-70, or FynT for 2 min at room temperature. Tyrosine phosphorylation of CasSD was analyzed as in (A).

(C) Extension-dependent phosphorylation of CasSD by c-Src measured by two different anti-phospho-Cas antibodies. Samples were prepared as in (A) except for the extent of the latex membrane stretching (40% in the left panel and 100% in the right panel). Equivalent portions of each sample were subjected to SDS-PAGE followed by pCas-165 and pCas-410 immunoblotting and avidin affinity blotting. Quantification of phosphorylation of CasSD was scaled with unextended NC-biotinylated CasSD set at 1 and noted below the anti-phospho-Cas blots with SD (n = 4).

reflection fluorescence (TIRF) or confocal microscope. Further, the stretchable substrate (silicone) had high background fluorescence. Therefore, we looked at αCas1 immunostaining of intact cells during the late phase of spreading on collagen-coated glass coverslips (20 min after plating), when the fast movement of actin cytoskeletons at the periphery is observed (Dubin-Thaler et al., 2004) and the forces required for continuous spreading are generated (Giannone et al., 2004). In RFP-Cas-expressing Cas-deficient fibroblasts, we found that αCas1 staining primarily colocalized with RFP-Cas in the peripheral regions (Figure 5C, top). An anti-phospho-Cas antibody (pCas-165) also exhibited a peripheral staining in the late spreading cells (Figure 5C, bottom), confirming that Cas extension correlated with phosphorylation. These staining patterns did not appear to be artifacts of antibody staining, since αCas3 staining always colocalized with RFP-Cas (Figure 5C, middle). Considering the specificity of αCas1 and αCas3 in immunoblotting (Figure S1C), both αCas1 and αCas3 staining most likely represent the distribution of their Cas epitopes, and not the crossreaction with other cellular protein(s). Indeed, we observed

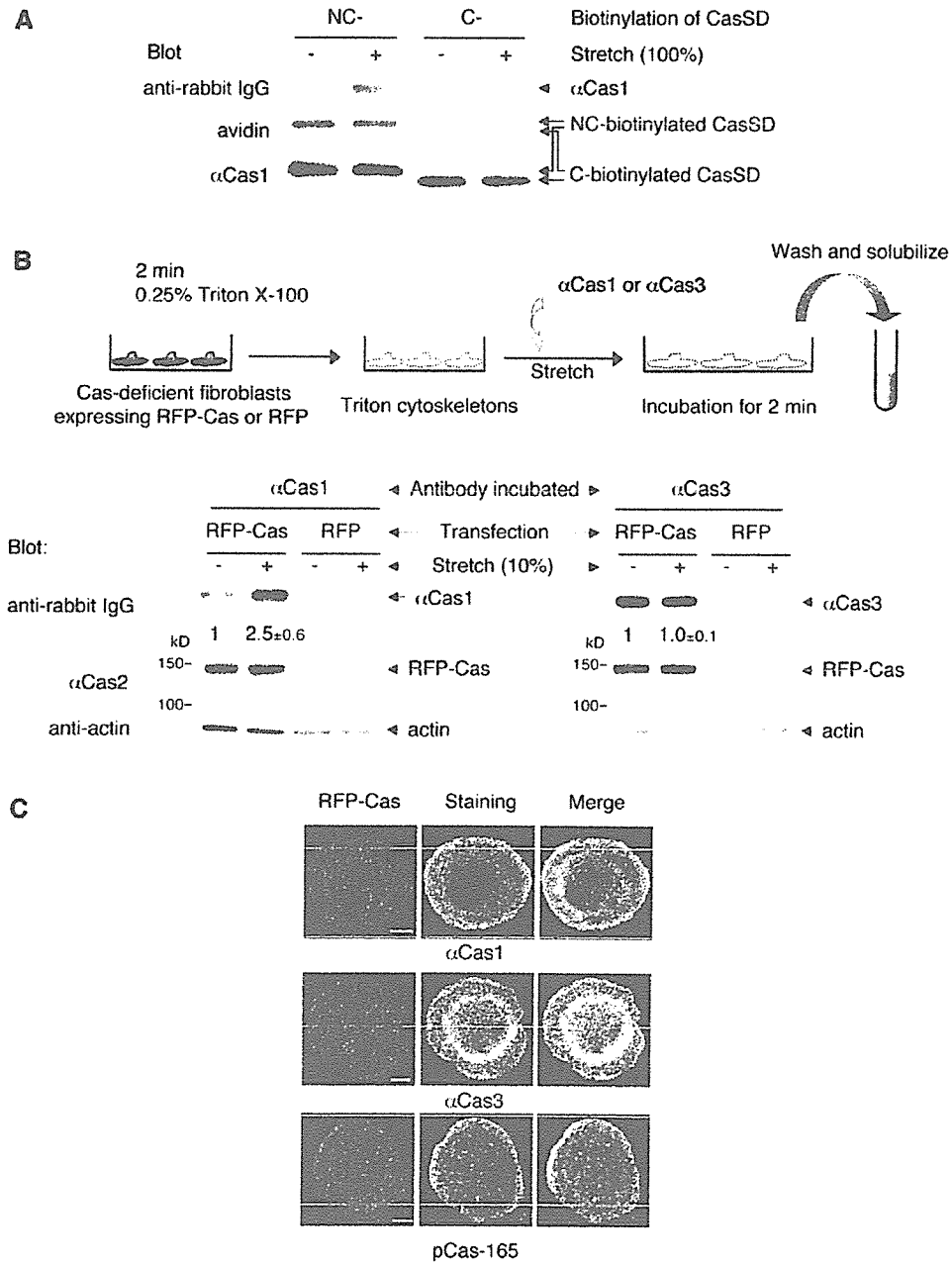

Figure 5. Extension of Cas In Situ and In Vivo

(A) αCas1 recognizes extended CasSD in vitro. NC-biotinylated or C-biotinylated CasSD was either extended (100%) or left unextended in the IPE system. After blocking, CasSD proteins were incubated with αCas1, washed, and solubilized with SDS sample buffer containing 0.12 M DTT. Equivalent portions of each sample were analyzed for quantification of bound αCas1 by anti-rabbit IgG immunoblotting. The amount of NC-biotinylated and C-biotinylated CasSD in each sample was quantified by avidin affinity blotting and αCas1 immunoblotting. Note that the difference in the relative signal intensity between avidin and αCas1 blots is consistent with the molar ratio of biotinylation (NC-biotinylated CasSD:C-biotinylated CasSD = 2:1).

(B) Stretch dependence of αCas1 and αCas3 binding to Cas in Triton cytoskeletons. Triton cytoskeletons were prepared from Cas-deficient fibroblasts transfected with RFP-Cas or RFP alone, either stretched or left unstretched, and incubated with either αCas1 or αCas3 as shown in the diagram. Quantification of bound antibody by anti-rabbit IgG immunoblotting was scaled with unstretched control set at 1 and noted with SD (n = 4).

(C) αCas1 preferentially binds to Cas, where higher traction forces are expected in vivo. Cas-deficient fibroblasts expressing RFP-Cas were plated, fixed after 20 min, and then stained with αCas1, αCas3, or pCas-165. Confocal images are shown for RFP-Cas (left, red channel) and immunostaining (center, green channel) and are merged on the right. Scale bars, 10 μm.

only faint background staining in untransfected Cas-deficient fibroblasts with either αCas1 or αCas3 (data not shown).

These in situ (cytoskeleton stretching) (Figure 5B) and in vivo (intact cell spreading) (Figure 5C) results, together with the observed preference of αCas1 binding for extended CasSD in vitro (Figure 5A), suggest that the in vitro extension of CasSD causes the conformational change of CasSD that is relevant to the force-dependent conformational change of Cas protein in vivo. Therefore, the extension-dependent phosphorylation of CasSD in vitro (Figure 4) appears to be relevant to the force-dependent phosphorylation of Cas in vivo (Figures 1, 2, and 5C).

DISCUSSION

Tyrosine Phosphorylation of Cas Is Involved in Physiological Force Transduction

Cas appears to act as a force transducer in vivo, since the knockdown of Cas expression by siRNA significantly attenuated stretch-dependent Rap1 activity (Figure 2A) and overexpression of wild-type Cas, but not coexpression of the phosphorylation-defective Cas mutant (Cas15YF) enhanced stretch-dependent Rap1 activity (Figure 2B). Phosphorylation by SFK is critical since stretch-dependent Cas phosphorylation was inhibited by the SFK inhibitor CGP77675 (Figure 1A) and attenuated in SYF cells (Figures 1B and 1C). These findings conform to our previous observation of stretch-dependent Cas phosphorylation by SFK in cytoskeletal complexes (Triton cytoskeletons) (Tamada et al., 2004) and indicate that tyrosine phosphorylation of Cas upon cell stretching constitutes a significant pathway for stretch-dependent Rap1 activation in intact cells (Sawada et al., 2001).

Possible Mechanisms for Stretch-Increased Cas Phosphorylation

Although Src was shown to be mechanically activated using genetically engineered reporters (Wang et al., 2005), it is not clear how endogenous c-Src is activated or if it is indirectly activated by force. We observed that Src-dependent phosphorylation of Cas was significantly increased by stretching in c-Src-expressing SYF cells without causing Src kinase activation (Figures 1B and 1C). These findings suggest that activation of the kinase is not primarily responsible for stretch-dependent increase of Cas phosphorylation in vivo. Since the SFK inhibitor greatly attenuated the stretch-dependent increase of Cas phosphorylation (Figure 1A), stretch-dependent alteration of phosphatase activity is also unlikely to be the cause. Further, the tyrosine phosphatase inhibitor sodium orthovanadate did not inhibit stretch-dependent tyrosine phosphorylation of Cas in Triton cytoskeletons (Tamada et al., 2004).

It is unlikely that stretching causes the spatial interaction between the kinase and the substrate, considering the constraints that such a mechanism places on the geometry of the cytoskeleton (Tamada et al., 2004). Since a mechanical modification of the substrate (Cas) was sufficient to increase Cas phosphorylation in vitro, we have focused on the analysis of that possibility.

Extension of Cas by Cellular Force

Both the amino-terminal SH3 and carboxy-terminal Src-binding domains are required for Cas localization at focal adhesions (Nakamoto et al., 1997), where cellular force is expected to be concentrated, and force-dependent signaling involving tyrosine phosphorylation occurs (Geiger and Bershadsky, 2002; Tamada et al., 2004). Since different proteins are known to associate with SH3 and Src-binding domains of Cas (Defilippi et al., 2006), an individual Cas molecule would be anchored to the cytoskeleton-adhesion complex via two distinct sites. In addition, the SH3 domain of Cas binds to FAK (focal adhesion kinase) (Harte et al., 1996). FAK has a FERM (erythrocyte band *4.1-ezrin-radixin-moesin*) domain commonly found in actin-binding proteins (Lee et al., 2004), associates with an actin-binding protein, talin (Chen et al., 1995), and is involved in the dynamic variation in tyrosine phosphorylation within focal adhesions (Ballestrem et al., 2006). Thus, we speculate that the amino-terminal anchor of Cas to the focal adhesion complex is more closely linked to the actin cytoskeleton than the carboxy-terminal anchor and that Cas is subjected to traction forces generated by the actin cytoskeleton (Figure 6).

Although the structures of the SH3 and the serine-rich domains of Cas were reported (Briknarova et al., 2005; Wisniewska et al., 2005), no structural analysis of the substrate domain has been reported, and the structure prediction algorithms (available at the Network Protein Sequence Analysis site) do not give a clear prediction for the structure of Cas substrate domain. We speculate that the intramolecular interactions within the substrate domain constrain its conformation in the absence of traction force and that traction force is required to expose YxxP sites to kinases.

Because our model centers on extension of Cas, the magnitude of force needed for extension is a concern. The force per integrin molecule in the adhesion site was estimated to be on the order of 1 pN (Balaban et al., 2001; Jiang et al., 2003), an order of magnitude below the force needed to reversibly unfold single domains of proteins such as spectrin by AFM (atomic force microscope) (Fisher et al., 1999). However, it has been shown that the protein unfolding force depends exponentially on the loading rate (Carrion-Vazquez et al., 1999), and at a low loading rate, proteins can be unfolded by forces even orders of magnitude below the forces required for unfolding at a high loading rate (Merkel et al., 1999). Further, extension of Cas may not require the force needed to cause "unfolding," i.e., linearization of a mechanically stable distinct structure. Thus, extension of Cas probably can occur by physiological forces at focal contact sites (order of a few pN). Further details of force-dependent extension and phosphorylation of the Cas substrate domain in vitro as well as in vivo are under study.

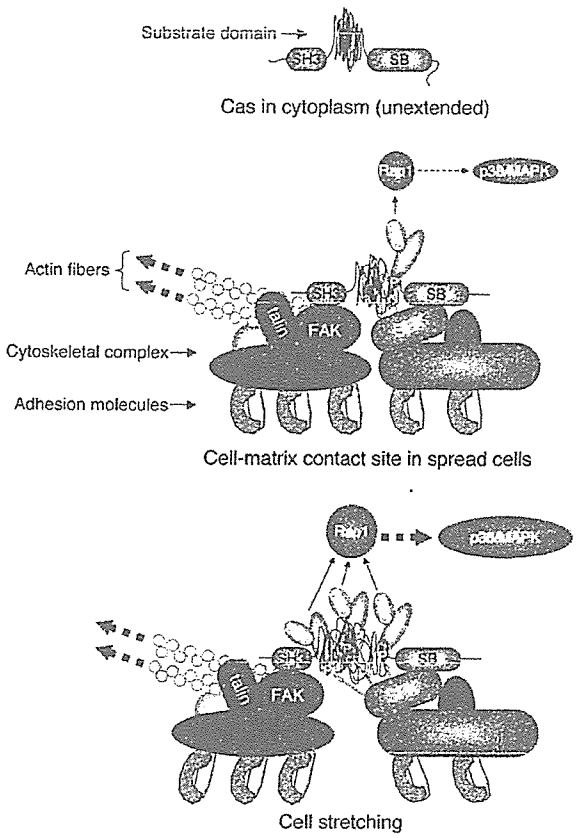

Figure 6. Model of Extension of Cas and Signaling at Cell-Matrix Contact Sites

The top and middle panels represent a Cas molecule with unextended configuration of substrate domain in the cytoplasm and a Cas molecule with moderate extension of substrate domain at the cell-matrix contact site of spread cells, respectively. The bottom panel represents the extension-dependent phosphorylation of the Cas substrate domain by SFK and enhancement of its downstream signaling. SH3 and SB represent the SH3- and the Src-binding domains of Cas, respectively.

Physiological Role of Extension and Phosphorylation of Cas in Force Transduction

Several different experimental approaches indicate that Cas extension plays a role in the direct sensing of traction forces in vivo. In vitro, extension of NC-biotinylated CasSD remarkably enhanced its phosphorylation by exogenous c-Src, FynT, or Abl1 (Figure 4). Extension of CaSD was confirmed by measuring the separation of two halves of YFP linked to the ends of the CasSD (Figure 3B). Stretch-dependent phosphorylation of Cas in cytoskeletons and in intact cells further supports the idea that it is involved in physiological force sensing. Antibody binding to epitopes exposed by extension in regions of higher traction forces shows that Cas is extended in vivo. Although many force-dependent effects are observed within cells, extension of Cas appears to be a primary force-sensing process and not part of a secondary force-response pathway, since extension-dependent phosphorylation of CasSD by active kinases was observed in vitro, where any extraneous biochemical interactions or signaling pathways were completely eliminated. While extracellular matrix proteins also respond to force by unfolding (Oberhauser et al., 2002) and exhibit different functional effects (Zhong et al., 1998), we show here that a cytoplasmic protein, Cas, has a gain of function upon cell stretching in terms of increase in phosphorylation and activation of Crk/C3G-Rap1 signaling.

A much greater percentage extension is required to observe the increase of in vitro phosphorylation of CasSD (Figure 4A, lanes 2–6) than the percentage of cell stretching to observe an increase of in vivo Cas phosphorylation (Figures 1 and 2). In vivo, cytoskeletal filaments will not stretch significantly, and cytoskeletal networks are believed to be strain hardened by cell-generated traction forces; therefore, molecular complexes at "stress-bearing" sites will be greatly extended upon even mild cell stretching. Moreover, cell traction forces will pre-extend the cytoskeleton-bound Cas molecules in spread cells even without stretching (Figure 6, middle). Thus, 10% stretching of intact cells can cause more than 10% extension of "unextended" Cas (Figure 6, top), since traction forces are concentrated at cell-matrix contact sites (Geiger and Bershadsky, 2002). In addition, αCas1 immunostaining shows that Cas is extended in the high-traction force regions of cells where Cas is phosphorylated (Figure 5C).

In other studies, shear stress increases Cas phosphorylation by SFK in vascular endothelial cells (Okuda et al., 1999). Since shear stress is known to modulate the cell contractility (Chien et al., 2005) in which Cas has been shown to play a role (Tang and Tan, 2003), extension of Cas caused by the increased cell contractility might result in shear stress-dependent phosphorylation. Thus, local extension of Cas is likely to be involved in the local response to various types of "mechanical stress" and can possibly account for the versatile function of Cas (Defilippi et al., 2006).

Substrate Priming as a General Mechanism of Cell Signaling

Enhancement of a substrate's susceptibility to phosphorylation by mechanical extension is designated as extension-dependent "substrate priming." The transduction of cell forces into a biochemical signal by mechanical substrate priming could be highly flexible and dynamic. The extent of substrate extension in vivo will depend upon the extent of strain produced locally in the cell, resulting in a graded extent of substrate phosphorylation and, consequently, gradations in the magnitude of downstream signaling events. Substrate priming by mechanical force might be generally involved in kinase signaling, particularly in light of our observation that a number of other cytoskeletal proteins are tyrosine phosphorylated in a stretch-dependent manner (Tamada et al., 2004) and since substrate conformation is a critical determinant in phosphorylation of other SFK substrates (Cooper et al., 1984). Thus, we suggest that substrate priming by localized protein

extension provides a simple mechanism for sensing the level of force on a cell as well as the location at which force is applied.

EXPERIMENTAL PROCEDURES

Antibodies

Polyclonal antibodies against Cas protein (αCas1, αCas2, and αCas3) were described previously (Sakai et al., 1994). The polyclonal anti-phospho-Cas antibodies pCas-165 and pCas-410, a polyclonal anti-phospho-SrcY416 antibody, and a polyclonal anti-phospho-SrcY527 antibody were purchased from Cell Signaling. The polyclonal anti-phospho-Cas antibody αP-Cas460Y (Miyake et al., 2005) was used for in vitro experiments with CasSD. Monoclonal anti-GFP (JL-8) and anti-RFP (anti-DsRed) antibodies were purchased from Clontech and BD Pharmingen, respectively. Monoclonal anti-Src (GD11) and anti-polyHistidine antibodies were purchased from Upstate Biotechnology and Sigma, respectively. Polyclonal anti-actin and anti-Rap1 antibodies were purchased from Santa Cruz Biotech.

Cells and DNA Plasmid Transfection

Human embryonic kidney (HEK) 293 cells, Cas-deficient fibroblasts (Huang et al., 2002), and SYF cells that lack c-Src, c-Yes, and Fyn were cultured in DMEM supplemented with 10% fetal bovine serum (FBS) and penicillin/streptomycin (100 IU/ml and 100 μg/ml) at 37°C and 5% CO_2. DNA plasmid transfection was performed with Fugene 6 (Roche) according to the manufacturer's protocol. To isolate stably transfected cell lines, pPUR that carried a puromycin-resistant gene (Clontech) was cotransfected, and clones were selected using puromycin (Clontech).

Immunoprecipitation and In Vitro Kinase Assay of Src

To measure the Src kinase activity in SYF cells and stable transfectant cells derived from SYF cells, Src was immunoprecipitated, and an in vitro kinase assay was performed using acid-treated enolase as a substrate. Phosphorylation of enolase was analyzed by anti-phospho-tyrosine immunoblotting. Details of the in vitro kinase assay of immunoprecipitated Src are described in the Supplemental Data section.

RNA Interference Experiments

To decrease the endogenous expression of Cas protein, two different siRNAs, BCAR1-HSS114272 and BCAR1-HSS114273 (Stealth RNAi, Invitrogen), were transfected into HEK293 cells (1×10^5/dish) using Lipofectamine RNAiMAX according to the manufacturer's protocol (180 pmol RNA interference [RNAi] and 9 μl Lipofectamine RNAiMAX/dish) (Invitrogen). Six hours after transfection, culture medium was replaced with fresh DMEM containing 10% FBS. Twenty-four hours after transfection, cells were either stretched or left unstretched and subjected to biochemical analyses.

Quantification of Rap1 Activity

A GST pull-down assay was performed to measure the Rap1 activity using GST-RalGDS-RBD that preferentially bound to Rap1·GTP (Sakakibara et al., 2002). To measure the Rap1 input, equivalent portions of each lysate were directly subjected to SDS-PAGE followed by immunoblotting.

Kinases and Substrates

Recombinant c-Src, FynT, Abl1, Csk, and ZAP-70 were purchased from Invitrogen. Specific kinase activities of c-Src, FynT, Csk, and ZAP-70 were determined by an in vitro kinase assay using poly-Glu/Tyr (4:1) as a substrate (Invitrogen). Abl1 kinase activity was determined by an in vitro kinase assay using Abl1 substrate (Invitrogen). Enolase (rabbit muscle) was purchased from Sigma. Bacterially expressed cdb3 was used as a substrate to measure the ZAP-70 activity.

Preparation of Biotinylated Proteins

Various forms of biotinylated CasSD were prepared using Biotin AviTag technology (Avidity). The Biotin AviTag sequence consists of 15 residues (GLNDIFEAQKIEWHE) and is specifically and efficiently biotinylated by the protein biotin ligase BirA. Biotinylated AviTag-fused proteins were obtained by coexpression with BirA in bacteria (BL21 Star, Invitrogen) cultured in NZCYM medium containing d-biotin (50 μM; Research Organics) at the time of IPTG induction. The molar ratio of biotin to AviTag-fused protein was confirmed to be 2:1 in NC-biotinylated CasSD and NY/CY-NC-biotinylated CasSD, and 1:1 in C-biotinylated CasSD and NY/CY-C-biotinylated CasSD. Details of biotinylated protein preparation are given in the Supplemental Data section.

For chimeric proteins of biotinylated CasSD and YFP components (NY/CY-NC-biotinylated CasSD and NY/CY-C-biotinylated CasSD), yellow fluorescence was observed and estimated in bacteria and in solution by quantitative fluorescence microscopy. Solutions containing NY/CY-NC-biotinylated CasSD or NY/CY-C-biotinylated CasSD were as fluorescent as solutions containing bacterially expressed full-length YFP at the same concentration (0.8 μM).

Plasmids

Plasmids used in this work are described in the Supplemental Data section.

Stretching of Intact Cells

Cells plated on collagen (type I; Sigma-Aldrich)-coated stretchable silicone dishes (Sawada et al., 2001) were either stretched biaxially (and kept stretched) or left unstretched in our cell stretching system (Sawada et al., 2001; Tamada et al., 2004).

Covalent Avidin Coating of Latex Membrane and Preparation of Biotinylated Proteins Specifically Bound to Avidin-Coated Latex Membrane

Avidin (Neutravidin) was covalently immobilized onto the surface of latex membrane by introducing the amine-reactive groups using Friedal-Crafts chemistry, and biotinylated proteins were bound to the immobilized avidin. Details of preparation of biotinylated protein bound to latex membrane are described in the Supplemental Data section.

IPE System

A biotinylated protein-bound latex membrane set in an adjustable tension ring was placed on a lubricated round-shaped glass stage and stretched biaxially and uniformly by pulling down the tension ring (Figure 3A, bottom). Magnitude of the latex membrane stretching was described as percent change of length in each dimension. For example, 100% stretching represented 2-fold expansion in each dimension. To recover the protein for analysis, the protein-bound membrane (Figure 3A, bottom) was incubated with 1× SDS sample buffer containing 0.12 M DTT at 95°C for 5 min. Using amine-reactive, photocleavable biotin analog (NHS-PC-LC-Biotin, PIERCE) (Sawada and Sheetz, 2002), we confirmed that this procedure recovered the majority (>95%) of biotinylated proteins bound to the immobilized avidin.

YFP Amino-Terminal Swapping Assay

NY/CY-NC-biotinylated, NY/CY-C-biotinylated (Figure 3B), or NC-biotinylated CasSD (Figure 3A) bound to avidin-coated latex membrane was prepared as described above. After stretching of latex membrane (100%) or without stretching, biotinylated CasSD proteins were washed two times with 1% BSA and 1% Triton X-100 in PBS and incubated with 2 μM His_6-YFP-N in 1% BSA and 1% Triton X-100 in PBS containing 1 mM DTT for 10 min at room temperature. The bound protein complex on the latex membrane was washed four times with 1% BSA and 1% Triton X-100 in PBS and two times with 1% Triton X-100 in PBS, recovered with 1× SDS sample buffer containing 0.12 M DTT. The samples were subjected to SDS-PAGE followed by anti-polyHistidine immunoblotting and avidin affinity blotting.

In Vitro Extension and Phosphorylation of CasSD

NC-biotinylated or C-biotinylated CasSD bound to avidin-coated latex membrane was prepared as described above. After stretching of latex membrane or without stretching, biotinylated CasSD proteins were washed three times with 0.25% Triton X-100 and 2% BSA in buffer A (20 mM HEPES [pH 7.5], 150 mM NaCl, 4 mM $MgCl_2$, 1 mM DTT, 1 mM PMSF, 20 μg/ml aprotinin, 0.5 mM EGTA) and three times with 0.1% BSA in buffer A and incubated with recombinant kinases (specific activity of each kinase used: 700 pmol/min phosphate transfer) in 350 μl of kinase reaction buffer (20 mM HEPES [pH 7.5], 0.9 mM ATP, 0.1% BSA, 140 mM NaCl, 10 mM $MgCl_2$, 3 mM $MnCl_2$, 0.5 mM EGTA, 20 μg/ml aprotinin, 1.5 mM DTT, 1.5 mM Na_3VO_4, 0.03% Brij-35) for 2 min at room temperature. After kinase reaction, biotinylated CasSD proteins were washed three times with ice-cold 1% Triton X-100 in PBS containing 1 mM Na_3VO_4, recovered, and solubilized by incubation with 1× SDS sample buffer containing 0.12 M DTT at 95°C for 5 min. Tyrosine phosphorylation of CasSD was determined by anti-phospho-Cas immunoblotting and avidin affinity blotting.

In Vitro Binding of αCas1 to Extended CasSD

NC-biotinylated or C-biotinylated CasSD bound to avidin-coated latex membrane was either extended (100%) or left unextended in PBS containing 1% Triton X-100, 2% BSA, 5% FBS, 1 mM DTT, 20 μg/ml aprotinin, and 0.5 mM EGTA. After 10 min, CasSD proteins on the latex surface were washed three times and incubated for 30 min with PBS containing 2% BSA, 5% FBS, 1 mM DTT, 20 μg/ml aprotinin, and 0.5 mM EGTA to block nonspecific binding and then incubated for 2 min with αCas1 diluted at 1:1200 in the same buffer. After six washes with PBS containing 0.1% Tween-20 and 1 mM DTT, bound proteins were solubilized with 1× SDS sample buffer containing 0.12 M DTT and subjected to SDS-PAGE followed by anti-rabbit IgG or αCas1 immunoblotting and avidin affinity blotting.

Binding of Two Different Anti-Cas Antibodies, αCas1 and αCas3, to Triton Cytoskeletons

Triton cytoskeletons were prepared from Cas-deficient fibroblasts transiently expressing RFP-Cas or RFP alone as described previously (Sawada and Sheetz, 2002). After two washes with buffer A containing 2% BSA and 5% FBS, the buffer was replaced with the buffer A containing 0.5 mM ATP, 2% BSA, 5% FBS, and either αCas1 or αCas3 (1:400 dilution), and Triton cytoskeletons were either stretched or left unstretched. After 2 min of incubation, samples were washed two times with buffer A containing 2% BSA and 5% FBS and four times with buffer A, solubilized with 1× SDS sample buffer containing 20 mM DTT, and subjected to SDS-PAGE followed by anti-rabbit IgG, αCas2, and anti-actin immunoblotting (Figure 5B, upper panel).

Immunofluorescence Staining, Fluorescence Microscopy, and Image Display

Twenty minutes after being plated on collagen (Type-I)-coated coverslips, Cas-deficient fibroblasts expressing RFP-Cas were washed with PBS; fixed with 3.7% formaldehyde in PBS; permeabilized with 0.1% Triton X-100 in PBS; stained using αCas1, αCas3, or pCas-165 as a primary antibody (1:400 dilution for αCas1 and αCas3 and 1:100 dilution for pCas-165) and Alexa Fluor 488 anti-rabbit IgG as a secondary antibody; and then viewed with a confocal microscope (Olympus IX-81 with FV500 system). Image intensity from the green channel (immunofluorescence with αCas1, αCas3, or pCas-165) and the red channel (RFP-Cas) was displayed with the contrast enhanced by setting the highest intensity in each image at the maximum value of the dynamic range and the background (cell-free area) at zero in ImageJ, a free open source Java imaging platform (http://rsb.info.nih.gov/ij/).

Statistical Analysis

Statistical analysis was performed with the paired Student's t test, and $p < 0.05$ was defined as significant.

Supplemental Data

The Supplemental Data include Supplemental Experimental Procedures and one supplemental figure and can be found with this article online at http://www.cell.com/cgi/content/full/127/5/1015/DC1/.

ACKNOWLEDGMENTS

We thank S. Ohkubo, T. Mandai, M. Cull, M. Galbmillion, and M.L. Bushey for assisting in the construction of the IPE system; P.S. Low, S.K. Hanks, T. Yamamoto, and M. Matsuda for the plasmids; J.M. Fernandez, M. Edidin, T.D. Perez, A. Sakakibara, C.D. Hu, H. Takayanagi, T. Miyazaki, T. Tezuka, M. Saitoh, K. Takeda, H. Ichijo, and K. Nakamura for helpful discussions and consistent support. This work was supported by NIH grant R01 EB001480.

Received: June 9, 2006
Revised: August 20, 2006
Accepted: September 25, 2006
Published: November 30, 2006

REFERENCES

Balaban, N.Q., Schwarz, U.S., Riveline, D., Goichberg, P., Tzur, G., Sabanay, I., Mahalu, D., Safran, S., Bershadsky, A., Addadi, L., and Geiger, B. (2001). Force and focal adhesion assembly: A close relationship studied using elastic micropatterned substrates. Nat. Cell Biol. *3*, 466–472.

Ballestrem, C., Erez, N., Kirchner, J., Kam, Z., Bershadsky, A., and Geiger, B. (2006). Molecular mapping of tyrosine-phosphorylated proteins in focal adhesions using fluorescence resonance energy transfer. J. Cell Sci. *119*, 866–875.

Bougeret, C., Rothhut, B., Jullien, P., Fischer, S., and Benarous, R. (1993). Recombinant Csk expressed in Escherichia coli is autophosphorylated on tyrosine residue(s). Oncogene *8*, 1241–1247.

Briknarova, K., Nasertorabi, F., Havert, M.L., Eggleston, E., Hoyt, D.W., Li, C., Olson, A.J., Vuori, K., and Ely, K.R. (2005). The serine-rich domain from Crk-associated substrate (p130Cas) is a four-helix bundle. J. Biol. Chem. *280*, 21908–21914.

Carrion-Vazquez, M., Oberhauser, A.F., Fowler, S.B., Marszalek, P.E., Broedel, S.E., Clarke, J., and Fernandez, J.M. (1999). Mechanical and chemical unfolding of a single protein: A comparison. Proc. Natl. Acad. Sci. USA *96*, 3694–3699.

Chen, H.C., Appeddu, P.A., Parsons, J.T., Hildebrand, J.D., Schaller, M.D., and Guan, J.L. (1995). Interaction of focal adhesion kinase with cytoskeletal protein talin. J. Biol. Chem. *270*, 16995–16999.

Chien, S., Li, S., Shiu, Y.T., and Li, Y.S. (2005). Molecular basis of mechanical modulation of endothelial cell migration. Front. Biosci. *10*, 1985–2000.

Cooper, J.A., Esch, F.S., Taylor, S.S., and Hunter, T. (1984). Phosphorylation sites in enolase and lactate dehydrogenase utilized by tyrosine protein kinases in vivo and in vitro. J. Biol. Chem. *259*, 7835–7841.

Defilippi, P., Di Stefano, P., and Cabodi, S. (2006). p130Cas: A versatile scaffold in signaling networks. Trends Cell Biol. *16*, 257–263.

Dubin-Thaler, B.J., Giannone, G., Dobereiner, H.G., and Sheetz, M.P. (2004). Nanometer analysis of cell spreading on matrix-coated surfaces reveals two distinct cell states and STEPs. Biophys. J. *86*, 1794–1806.

Fisher, T.E., Oberhauser, A.F., Carrion-Vazquez, M., Marszalek, P.E., and Fernandez, J.M. (1999). The study of protein mechanics with the atomic force microscope. Trends Biochem. Sci. *24*, 379–384.

Fonseca, P.M., Shin, N.Y., Brabek, J., Ryzhova, L., Wu, J., and Hanks, S.K. (2004). Regulation and localization of CAS substrate domain tyrosine phosphorylation. Cell. Signal. *16*, 621–629.

Geiger, B., and Bershadsky, A. (2002). Exploring the neighborhood: Adhesion-coupled cell mechanosensors. Cell *110*, 139–142.

Giannone, G., and Sheetz, M.P. (2006). Substrate rigidity and force define form through tyrosine phosphatase and kinase pathways. Trends Cell Biol. *16*, 213–223.

Giannone, G., Dubin-Thaler, B.J., Dobereiner, H.G., Kieffer, N., Bresnick, A.R., and Sheetz, M.P. (2004). Periodic lamellipodial contractions correlate with rearward actin waves. Cell *116*, 431–443.

Harte, M.T., Hildebrand, J.D., Burnham, M.R., Bouton, A.H., and Parsons, J.T. (1996). p130Cas, a substrate associated with v-Src and v-Crk, localizes to focal adhesions and binds to focal adhesion kinase. J. Biol. Chem. *271*, 13649–13655.

Hattori, M., and Minato, N. (2003). Rap1 GTPase: Functions, regulation, and malignancy. J. Biochem. (Tokyo) *134*, 479–484.

Hu, C.D., Chinenov, Y., and Kerppola, T.K. (2002). Visualization of interactions among bZIP and Rel family proteins in living cells using bimolecular fluorescence complementation. Mol. Cell *9*, 789–798.

Huang, J., Hamasaki, H., Nakamoto, T., Honda, H., Hirai, H., Saito, M., Takato, T., and Sakai, R. (2002). Differential regulation of cell migration, actin stress fiber organization, and cell transformation by functional domains of Crk-associated substrate. J. Biol. Chem. *277*, 27265–27272.

Isakov, N., Wange, R.L., Watts, J.D., Aebersold, R., and Samelson, L.E. (1996). Purification and characterization of human ZAP-70 protein-tyrosine kinase from a baculovirus expression system. J. Biol. Chem. *271*, 15753–15761.

Jiang, G., Giannone, G., Critchley, D.R., Fukumoto, E., and Sheetz, M.P. (2003). Two-piconewton slip bond between fibronectin and the cytoskeleton depends on talin. Nature *424*, 334–337.

Katsumi, A., Milanini, J., Kiosses, W.B., del Pozo, M.A., Kaunas, R., Chien, S., Hahn, K.M., and Schwartz, M.A. (2002). Effects of cell tension on the small GTPase Rac. J. Cell Biol. *158*, 153–164.

Klinghoffer, R.A., Sachsenmaier, C., Cooper, J.A., and Soriano, P. (1999). Src family kinases are required for integrin but not PDGFR signal transduction. EMBO J. *18*, 2459–2471.

Lee, H.S., Bellin, R.M., Walker, D.L., Patel, B., Powers, P., Liu, H., Garcia-Alvarez, B., de Pereda, J.M., Liddington, R.C., Volkmann, N., et al. (2004). Characterization of an actin-binding site within the talin FERM domain. J. Mol. Biol. *343*, 771–784.

Mayer, B.J., Hirai, H., and Sakai, R. (1995). Evidence that SH2 domains promote processive phosphorylation by protein-tyrosine kinases. Curr. Biol. *5*, 296–305.

Merkel, R., Nassoy, P., Leung, A., Ritchie, K., and Evans, E. (1999). Energy landscapes of receptor-ligand bonds explored with dynamic force spectroscopy. Nature *397*, 50–53.

Missbach, M., Jeschke, M., Feyen, J., Muller, K., Glatt, M., Green, J., and Susa, M. (1999). A novel inhibitor of the tyrosine kinase Src suppresses phosphorylation of its major cellular substrates and reduces bone resorption in vitro and in rodent models in vivo. Bone *24*, 437–449.

Miyake, I., Hakomori, Y., Misu, Y., Nakadate, H., Matsuura, N., Sakamoto, M., and Sakai, R. (2005). Domain-specific function of ShcC docking protein in neuroblastoma cells. Oncogene *24*, 3206–3215.

Nakamoto, T., Sakai, R., Honda, H., Ogawa, S., Ueno, H., Suzuki, T., Aizawa, S., Yazaki, Y., and Hirai, H. (1997). Requirements for localization of p130cas to focal adhesions. Mol. Cell. Biol. *17*, 3884–3897.

Oberhauser, A.F., Badilla-Fernandez, C., Carrion-Vazquez, M., and Fernandez, J.M. (2002). The mechanical hierarchies of fibronectin observed with single-molecule AFM. J. Mol. Biol. *319*, 433–447.

Okuda, M., Takahashi, M., Suero, J., Murry, C.E., Traub, O., Kawakatsu, H., and Berk, B.C. (1999). Shear stress stimulation of p130(cas) tyrosine phosphorylation requires calcium-dependent c-Src activation. J. Biol. Chem. *274*, 26803–26809.

Rief, M., Gautel, M., Oesterhelt, F., Fernandez, J.M., and Gaub, H.E. (1997). Reversible unfolding of individual titin immunoglobulin domains by AFM. Science *276*, 1109–1112.

Sakai, R., Iwamatsu, A., Hirano, N., Ogawa, S., Tanaka, T., Mano, H., Yazaki, Y., and Hirai, H. (1994). A novel signaling molecule, p130, forms stable complexes in vivo with v-Crk and v-Src in a tyrosine phosphorylation-dependent manner. EMBO J. *13*, 3748–3756.

Sakakibara, A., Ohba, Y., Kurokawa, K., Matsuda, M., and Hattori, S. (2002). Novel function of Chat in controlling cell adhesion via Cas-Crk-C3G-pathway-mediated Rap1 activation. J. Cell Sci. *115*, 4915–4924.

Sawada, Y., and Sheetz, M.P. (2002). Force transduction by Triton cytoskeletons. J. Cell Biol. *156*, 609–615.

Sawada, Y., Nakamura, K., Doi, K., Takeda, K., Tobiume, K., Saitoh, M., Morita, K., Komuro, I., De Vos, K., Sheetz, M., and Ichijo, H. (2001). Rap1 is involved in cell stretching modulation of p38 but not ERK or JNK MAP kinase. J. Cell Sci. *114*, 1221–1227.

Shin, N.Y., Dise, R.S., Schneider-Mergener, J., Ritchie, M.D., Kilkenny, D.M., and Hanks, S.K. (2004). Subsets of the major tyrosine phosphorylation sites in Crk-associated substrate (CAS) are sufficient to promote cell migration. J. Biol. Chem. *279*, 38331–38337.

Tamada, M., Sheetz, M.P., and Sawada, Y. (2004). Activation of a signaling cascade by cytoskeleton stretch. Dev. Cell *7*, 709–718.

Tang, D.D., and Tan, J. (2003). Role of Crk-associated substrate in the regulation of vascular smooth muscle contraction. Hypertension *42*, 858–863.

Thomas, S.M., and Brugge, J.S. (1997). Cellular functions regulated by Src family kinases. Annu. Rev. Cell Dev. Biol. *13*, 513–609.

Vogel, V., and Sheetz, M. (2006). Local force and geometry sensing regulate cell functions. Nat. Rev. Mol. Cell Biol. *7*, 265–275.

Wang, Y., Botvinick, E.L., Zhao, Y., Berns, M.W., Usami, S., Tsien, R.Y., and Chien, S. (2005). Visualizing the mechanical activation of Src. Nature *434*, 1040–1045.

Wisniewska, M., Bossenmaier, B., Georges, G., Hesse, F., Dangl, M., Kunkele, K.P., Ioannidis, I., Huber, R., and Engh, R.A. (2005). The 1.1 A resolution crystal structure of the p130cas SH3 domain and ramifications for ligand selectivity. J. Mol. Biol. *347*, 1005–1014.

Zhong, C., Chrzanowska-Wodnicka, M., Brown, J., Shaub, A., Belkin, A.M., and Burridge, K. (1998). Rho-mediated contractility exposes a cryptic site in fibronectin and induces fibronectin matrix assembly. J. Cell Biol. *141*, 539–551.

Molecular Mechanism of the Life and Death of the Osteoclast

SAKAE TANAKA, TSUYOSHI MIYAZAKI, AKIRA FUKUDA, TORU AKIYAMA, YUHO KADONO, HIDETOSHI WAKEYAMA, SHINJIRO KONO, SHINYA HOSHIKAWA, MASAKI NAKAMURA, YASUSHI OHSHIMA, ATSUHIKO HIKITA, ICHIRO NAKAMURA, AND KOZO NAKAMURA

Department of Orthopaedic Surgery, Faculty of Medicine, The University of Tokyo, Tokyo 113-0033, Japan

ABSTRACT: **The life span of osteoclasts is critically regulated by various cytokines, and therapeutics such as bisphosphonates act directly on osteoclasts and induce apoptosis of the cells. This article will focus on the molecular mechanism of osteoclast apoptosis and summarize the recent advances in this field with an emphasis on the role of intracellular signaling pathways.**

KEYWORDS: **osteoclast; cytokines; apoptosis; Akt; TNF; Rac1; Bim**

THE ROLE OF APOPTOSIS IN BONE HOMEOSTASIS

The homeostasis of the skeletal tissues is maintained by a well-organized regulation of bone formation and bone resorption. This process is called remodeling, in which osteoblasts are mainly involved in the bone formation process and osteoclasts are essential for bone resorption. Osteoclasts are terminally differentiated cells primarily involved in physiological and pathological bone resorption. The life span of osteoclasts is relatively short both *in vitro* and *in vivo*, and once differentiated, they rapidly die in the absence of supporting cells such as osteoblasts or bone marrow stromal cells, or growth factors, such as interleukin (IL)-1, receptor activator of NF-κB ligand (RANKL), and macrophage colony-stimulating factor (M-CSF).[1] Antiresorptive drugs such as estrogen, raloxifene, and bisphosphonates are known to reduce the life span of osteoclasts.[2]

Recent studies have revealed that the rapid cell death of osteoclasts is caused by apoptosis. Apoptosis is a form of programmed cell death that is characterized

Address for correspondence: Sakae Tanaka, Department of Orthopaedic Surgery, Faculty of Medicine, The University of Tokyo, 7-3-1 Hongo, Bunkyo-ku, Tokyo 113-0033, Japan. Voice: 81-3-3815-5411 ext 33376; fax: 81-3-3818-4082.
e-mail: TANAKAS-ORT@h.u-tokyo.ac.jp

Ann. N.Y. Acad. Sci. 1068: 180–186 (2006).
doi: 10.1196/annals.1346.020

by specific morphological and biochemical properties.[3,4] Morphologically, apoptosis is characterized by a series of structural changes in dying cells: blebbing of the plasma membrane, condensation of the cytoplasm and the nucleus, and cellular fragmentation into membrane apoptotic bodies. Biochemically, apoptosis is characterized by the degradation of chromatin, initially into large fragments of 50–300 kilobases and subsequently into smaller fragments that are monomers and multimers of 200 bases.[4,5] Not only does apoptosis regulate various aspects of the biological activity but also can trigger cancer, autoimmune diseases, and degenerative disorders.

INTRACELLULAR SIGNALING PATHWAYS REGULATING OSTEOCLAST SURVIVAL

Using adenovirus vector-mediated gene transduction system, we found that the activation of extracellular-regulating kinase (Erk) by transducing a constitutively active mutant of Mek1 markedly promoted the survival of osteoclasts.[6] Conversely, inhibiting Erk activation by overexpressing a dominant negative *ras* gene mutant rapidly induced apoptotic cell death of the cells.[6] These results, combined with the fact that anti-apoptotic factors such as RANKL, IL-1, and M-CSF also induce Erk activation in osteoclasts, suggest that the Ras-Erk pathway plays an essential role in osteoclast survival.

Recent studies have revealed the critical role of phosphatidylinositol 3-kinase (PI3K)/Akt pathways in the survival of osteoclasts. Xing *et al.* reported that the transgenic overexpression of Src251, which contains SH2 and SH3 domains of chicken c-Src but lacks the kinase domain, under the control of the tartrate-resistant acid phosphatase (TRAP) promotor induced osteopetrosis in mice.[7] The mice had a reduced number of osteoclasts, and osteoclasts of Src251 transgenic mice showed apoptotic phenotypes. The activity of Akt in the Src251 transgenic mouse osteoclasts was significantly reduced, and the RANKL-induced Akt activation was impaired in the cells, suggesting that Akt plays a critical role in osteoclast survival, and Akt activation is at least partly mediated by c-Src.[7] Using a mouse osteoclast formation system, Lee *et al.* showed that tumor necrosis factor-α (TNF-α) prolonged the survival of osteoclasts, which was abrogated by either PI3K inhibitors or Mek/Erk inhibitors.[8] They also revealed the involvement of Grb2 and ceramide in TNF-α-induced Erk activation in osteoclasts.[8] A similar effect was observed in IL-1α.[9] Glantschnig *et al.* exhibited the central role of mTOR/S6K pathways in M-CSF- and RANKL-induced osteoclast survival, which was suppressed by rapamycin.[10] We also found that the adenovirus vector-mediated overexpression of constitutively active Akt stimulates osteoclast survival (Fukuda *et al.*, unpublished observation). These results clearly suggest the crucial role of Akt pathways on the osteoclast survival. However, contrary to these previous observations, Sugatani and Ross recently reported that silencing of Akt1

and/or Akt2 by small interfering RNA (siRNA) suppressed osteoclast differentiation but did not affect osteoclast survival.[11] The reason of this discrepancy remains unknown, and further investigation is required to clarify the exact role of PI3K/Akt pathways in the osteoclast survival.

Rac1 is a member of the Rho family small G-proteins and recent studies have revealed that it mediates anti-apoptotic signals in some types of cells. Rac1 is reported to be required for the cytoskeletal organization and bone-resorbing activity of osteoclasts, but its role in the osteoclast survival and function is not fully elucidated yet. To examine the role of Rac1 in the osteoclast survival and function, we examined the effect of dominant negative Rac1 and constitutively active Rac1 expression on osteoclasts.[12] Adenovirus vector-mediated dominant negative Rac1 ($Rac1^{DN}$) expression significantly reduced the pit formation of osteoclasts, and promoted their apoptosis. M-CSF rapidly activated Rac1, consistent with the results reported by Faccio *et al.*,[13] and the pro-survival effect of M-CSF for osteoclasts was abrogated by $Rac1^{DN}$ overexpression. Constitutively active Rac1 enhanced osteoclast survival, which was completely suppressed by PI3K inhibitors, while Mek inhibitors had only partial effects. Using time-lapse video-microscopy, we found that $Rac1^{DN}$ expression reduced the membrane ruffling and spreading of osteoclasts in response to M-CSF. These results strongly suggest that small GTPase Rac1 is critically involved in M-CSF receptor signaling, and mediates survival signaling of osteoclasts primarily by modulating PI3K/Akt pathways. Faccio *et al.* recently demonstrated that a guanine nucleotide exchange factor Vav3 lies upstream of Rac1 activation in osteoclasts, and is involved in the signaling of M-CSF receptor and $\alpha v\beta 3$ integrin.[14]

ROLE OF BCL-2 FAMILY MEMBERS IN OSTEOCLAST APOPTOSIS

The apoptotic process can be divided into two different pathways, the extrinsic (death receptor) pathway and the intrinsic (mitochondrial) pathway.[15] In the death receptor pathway, the activation of a receptor belonging to the TNF receptor family leads to the induction of apoptosis through the activation of aspartate-specific cystein proteases (caspases) 8, and the anti- and pro-apoptotic Bcl-2 family members are critically involved in the intrinsic pathway by regulating cytochrome *c* release from the mitochondrial intermembrane into the cytosol, which leads to the activation of caspase 9.[15] The anti-apoptotic members include mammalian Bcl-2, Bcl-x_L, Bcl-w, Mcl-1, A1, and *C. elegans* CED-9. So far, more than 20 members of pro-apoptotic Bcl-2 family proteins have been identified in mammals, and they can be further divided into two groups; multi-domain members possessing homology in BH1-3 domains and BH3 domain-only members. Multi-domain members include Bax, Bak, Bok and *D. melanogaster* DEBCL/DROB, and BH3-only members include

mammalian Bad, Bik/Nbk, Bid, Hrk/DP5, Blk, Bim, Noxa and *C. elegans* EGL-1.[16] It was recently reported that BH3-only proteins failed to induce cytochrome *c* release and apoptosis in *bax-/-bak-/-* cells, suggesting that Bax-like proteins mediate death signals from various BH3-only proteins.[17] Bax-like proteins are ubiquitously expressed, while BH3-only members have a more tissue-specific distribution, indicating that the latter may play a role in the tissue/cell-specific regulation of apoptosis.

The activity of BH3-only proteins is strictly regulated to prevent unorganized cell death. The expression of Noxa is induced by p53 or IRF-1, and DP5/Hrk is transcriptionally upregulated in the absence of growth factors or when the cells are exposed to β-amyloid protein. The other mechanism regulating their activity is the posttranslational modification. It is now widely recognized that Bad is phosphorylated at various sites and sequestrated away from Bcl-2 family members by binding to 14-3-3.[18,19] Many kinases including Akt, mitochondrial-anchored protein kinase A, Pak1, Rsk and Raf1, and phosphatase calcineurin have been reported to modify Bad, although the physiological importance of these regulations still remains unclear.

Depolarization of mitochondrial transmembrane potential, chromatin condensation, and cytochrome *c* release from mitochondria into cytoplasm were observed in the apoptotic osteoclasts, implying that cytokine deprivation triggers osteoclast apoptosis through the mitochondrial pathway.

A possible role of anti-apoptotic Bcl-2 family members for osteoclast survival has been reported. Okahashi *et al.*[20] showed that M-CSF treatment increased Bcl-2 mRNA expression in osteoclasts, and we found that adenovirus vector-mediated overexpression of Bcl-xL markedly prolonged survival of the cells *in vitro*.[21] Roodman and co-workers developed a transgenic mouse, in which Bcl-xL together with Simian Virus 40 large T antigen were specifically overexpressed in osteoclasts under the control of the TRAP promotor, and successfully established an immortalized osteoclast precursor cell line from the mice.[22] These results clearly showed that anti-apoptotic Bcl-2 family proteins play important roles in osteoclast survival both *in vitro* and *in vivo*. The mechanism regulating Bcl-2 and Bcl-xL expression in osteoclasts has not been clarified yet, but McGill *et al.* showed that Bcl-2 expression is regulated by Mitf, a transcription factor essential for osteoclast and melanocytes development.[23]

PRO-APOPTOTIC BH3-ONLY PROTEIN BIM IS INVOLVED IN OSTEOCLAST APOPTOSIS

Bim, one of the BH3-only proteins, was first identified as a Bcl-2 interacting protein by screening a λ-phage expression library constructed from a mouse thymic lymphoma.[24] Bim is expressed in hematopoietic, epithelial, neuronal, and germ cells,[25] and alternative splicing generates various Bim isoforms.

including Bim_S, Bim_L, and Bim_{EL}. Bim has been shown to play an essential role in the induction of apoptosis in T lymphocytes, B lymphocytes, and neurons, mainly based on the finding in Bim-deficient animals,[26,27] and its activity is also regulated both transcriptionally and posttranscriptionally.[28] The expression of Bim is downregulated at the transcriptional level by IL-3 signaling through Raf/Erk pathways and/or PI3K/mammalian target of rapamycin (mTOR) pathways in IL-3-dependent Ba/F3 cells.[29] The transcription of Bim is also upregulated in neonatal sympathetic neurons in response to the nerve growth factor deprivation. In healthy cells, Bim_L is bound to LC8, a component of the microtubule-associated dynein motor complex, and is sequestered to this complex in the cytoplasm. Certain apoptosis stimuli induce dissociation of this complex, and allow the translocation of Bim_L-LC8 complex to Bcl-xL on the mitochondrial membrane.[28]

We demonstrated a novel and unique regulation of apoptosis by ubiquitylation-dependent degradation of Bim in osteoclasts.[21] In the presence of M-CSF, Bim is constitutively ubiquitylated and degraded, and cytokine deprivation induced rapid upregulation of Bim due to the reduced level of its ubiquitylation.[21] C-Cbl is a possible candidate of E3 ubiquitin ligase of Bim in osteoclasts because Bim ubiquitylation was reduced in c-Cbl-deficient osteoclasts. Bim-deficient osteoclasts exhibited prolonged survival both *in vitro* and *in vivo*, and however, their bone-resorbing activity was significantly reduced, consistent with the *in vivo* observation that *bim–/–* animals showed mild osteosclerosis.[21] Consistent with our observation, Sugatani and Hruska reported that silencing the *bim* gene by siRNA prolonged the survival of osteoclasts.[11] These results clearly demonstrate that pro-apoptotic protein Bim plays a crucial role in osteoclast apoptosis and activation. Further studies are required to elucidate the mechanism of action and the regulation of Bim in osteoclasts, and the role of Bim in skeletal disorders.

CONCLUSIONS AND PERSPECTIVES

The success of bisphosphonates as the therapeutics of osteoporosis, together with the finding that bisphosphonates act directly on osteoclasts to induce their apoptosis, has attracted a great deal of attention to the molecular mechanism of osteoclast apoptosis, and remarkable progress has been made during the last several years to reveal the signaling pathways involved in the process. Therapeutics targeting these signaling pathways (molecules) will provide a novel treatment for bone diseases.

ACKNOWLEDGMENTS

This work was in part supported by Grants-in-Aid from the Ministry of Education, Culture, Sports, Science and Technology of Japan and Health Science